

## INFORMATION TO USERS

The most advanced technology has been used to photograph and reproduce this manuscript from the microfilm master. UMI films the text directly from the original or copy submitted. Thus, some thesis and dissertation copies are in typewriter face, while others may be from any type of computer printer.

The quality of this reproduction is dependent upon the quality of the copy submitted. Broken or indistinct print, colored or poor quality illustrations and photographs, print bleedthrough, substandard margins, and improper alignment can adversely affect reproduction.

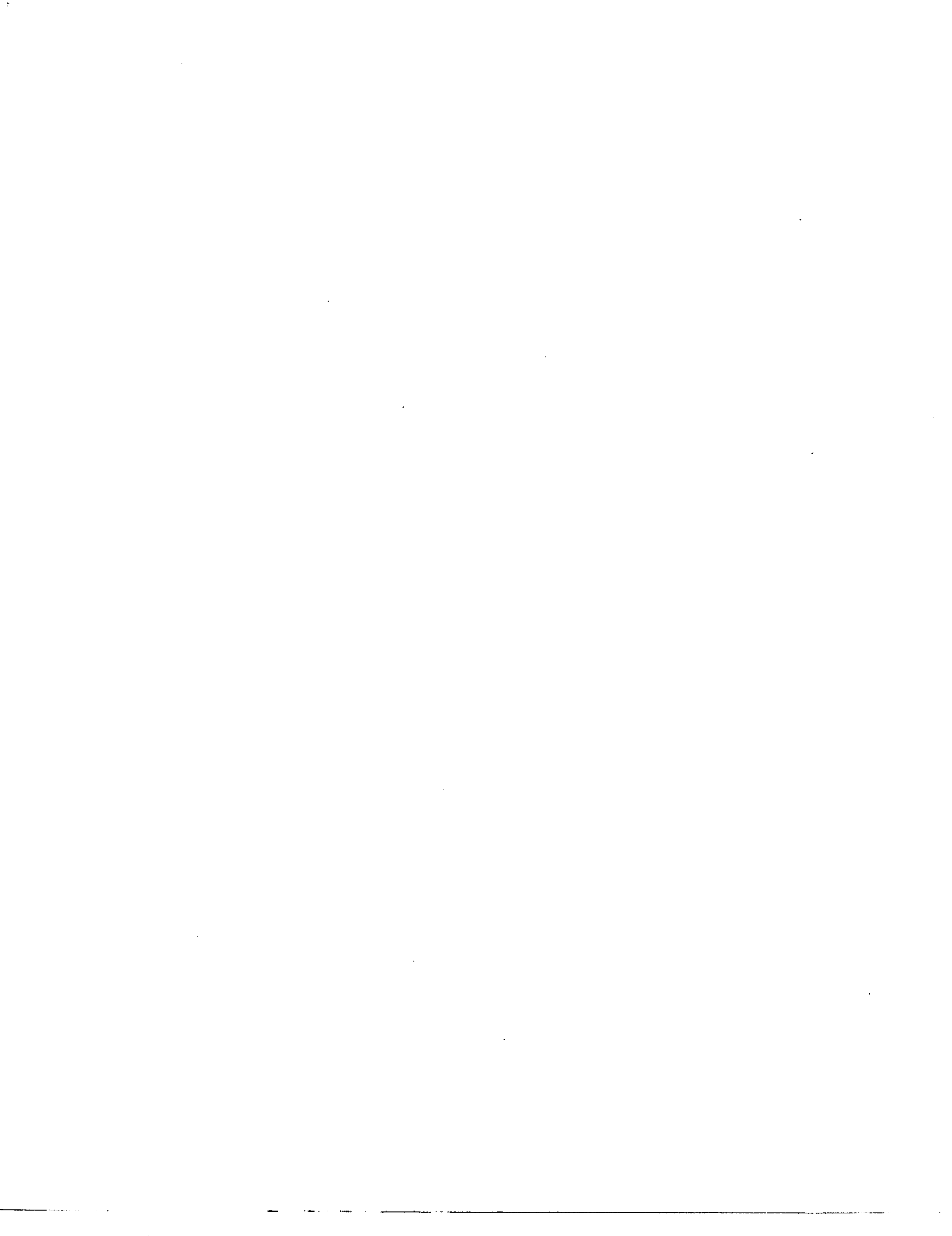
In the unlikely event that the author did not send UMI a complete manuscript and there are missing pages, these will be noted. Also, if unauthorized copyright material had to be removed, a note will indicate the deletion.

Oversize materials (e.g., maps, drawings, charts) are reproduced by sectioning the original, beginning at the upper left-hand corner and continuing from left to right in equal sections with small overlaps. Each original is also photographed in one exposure and is included in reduced form at the back of the book. These are also available as one exposure on a standard 35mm slide or as a 17" x 23" black and white photographic print for an additional charge.

Photographs included in the original manuscript have been reproduced xerographically in this copy. Higher quality 6" x 9" black and white photographic prints are available for any photographs or illustrations appearing in this copy for an additional charge. Contact UMI directly to order.

# U·M·I

University Microfilms International  
A Bell & Howell Information Company  
300 North Zeeb Road, Ann Arbor, MI 48106-1346 USA  
313/761-4700 800/521-0600



**Order Number 1335389**

**Dilatancy effects on the constitutive modeling of granular soils**

**Salahuddin, Mohammed, M.S.**

**The University of Arizona, 1988**

**U·M·I**

**300 N. Zeeb Rd.  
Ann Arbor, MI 48106**



**DILATANCY EFFECTS ON THE CONSTITUTIVE  
MODELING OF GRANULAR SOILS**

by

**Mohammed Salahuddin**

---

A Thesis Submitted to the Faculty of the  
**DEPARTMENT OF CIVIL ENGINEERING AND ENGINEERING MECHANICS**  
In Partial Fulfillment of the Requirements  
For the Degree of  
**MASTER OF SCIENCE**  
**WITH A MAJOR IN CIVIL ENGINEERING**  
In the Graduate College  
**THE UNIVERSITY OF ARIZONA**

1 9 8 8

STATEMENT BY AUTHOR

This thesis has been submitted in partial fulfillment of requirements for an advanced degree at The University of Arizona and is deposited in the University Library to be made available to borrowers under rules of the Library.

Brief quotations from this thesis are allowable without special permission, provided that accurate acknowledgement of source is made. Request for permission for extended quotation from or reproduction of this manuscript in whole or part may be granted by the head of the major department or the Dean of the Graduate College when in his or her judgment the proposed use of the material is in the interests of scholarship. In all other instances, however, permission must be obtained from the author.

SIGNED: Md. Salahuddin.

APPROVAL BY THESIS DIRECTOR

The Thesis has been approved on the date shown below:

Panos D. Kiousis

Dr. Panos D. Kiousis  
Assistant Professor of Civil Engineering  
and Engineering Mechanics

8/31/88

Date

## ACKNOWLEDGMENTS

The author expresses his respect to Professor Panos D. Kiouisis who directed the thesis work with sincere devotion and constructive criticism, and thanks Professor E. Nowatzki for his comments. Due respect also to Professor A. M. M. Safiullah (Bangladesh University of Engineering and Technology) who encouraged the author to pursue his studies in the Geotechnical Engineering field.

## TABLE OF CONTENTS

	Page
ABSTRACT	v
CHAPTER	
1. INTRODUCTION	1
2. SCOPE AND OBJECTIVE	3
3. LITERATURE REVIEW	4
3.1 General	4
3.2 Some fundamentals of plasticity Theory	7
3.2.1 Yield criterion	8
3.2.2 Normality rule	10
3.2.3 Stress-Elastic Strain Relationship	11
3.3 Evolution or hardening rule	12
3.3.1 Classification of hardening rules	13
3.3.1.1 Isotropic hardening	13
3.3.1.2 Kinematic hardening	14
3.3.1.3 Anisotropic hardening	14
4. TEST PROGRAM	16
4.1 General	16
4.2 Description of test procedure	16
4.3 Types of Consolidated, Drained Triaxial tests	22
4.4 Results of tests	25
4.5 Summary of test results	55
5. COMPARISON WITH PUBLISHED LITERATURE	57
5.1 General	57
5.2 Comparison and Conclusions	71
6. SUMMARY AND CONCLUSIONS	75
LIST OF REFERENCES	77

## ABSTRACT

Unique features of behavior of granular materials make constitutive modeling of these materials a challenge that has not yet been answered completely. Because volume changes are so important for the type of behavior exhibited by frictional materials, it is important to correctly incorporate them in constitutive models, both in terms of their rate of development and their magnitude.

In this study a number of consolidated drained triaxial tests are performed to find those features of sand behavior that can be considered "material parameters" and can be used for constitutive modeling of granular soils. Special attention is given to those features of material behavior that are related to dilatancy. A number of published experimental data are also analyzed and useful trends of soil behavior are found.

## 1. INTRODUCTION

The progress in the analysis of soil-structure systems using elastic stress-strain models has been seriously limited by difficulties in modeling several important features of the soil behavior. Not all granular materials behave the same way, therefore, it is difficult to model them. While general stress-strain non-linearity could be incorporated into elastic models in a satisfactory manner, the features associated with stress path dependency and dilatancy are much more difficult to deal with.

Granular materials display some unique features of behavior. These features make constitutive modeling of these materials a challenge that has not yet been answered completely. Plasticity theory, is one of the most popular contemporary approaches for developing non linear constitutive relations of geologic materials. Plasticity models for granular materials have to account for some "unusual" material properties such as shear dilatancy and pressure sensitivity. These properties are explained briefly in the following.

Granular materials exhibit significant volume changes during shear. In general, loose sand compresses and dense sand dilates (increases in volume) during triaxial compression. If the confining pressure is large however, even dense sand tends to compress mainly due to particle crushing. Also if the pressure is very low, even loose sand tends to dilate. These volume changes, whether compression or dilation, can attain substantial magnitudes and account in a rather sensitive manner for many of the behavior patterns associated with frictional materials. Dense granular materials exhibit a high rate of dilation under drained conditions and the stress-strain relation is smoothly curved. In comparison, volume changes

are completely prevented during undrained loading of granular materials. Because their tendency for dilation is prevented, suction or decrease in pore pressure occurs. This results in equal increase of effective confining pressure and a corresponding increase in strength. If cavitation of pore fluid is avoided by using a high back pressure, the effective confining pressure can increase substantially, and the undrained strength can be several times higher than the drained strength (for dilating materials).

Because volume changes are so important for the type of behavior exhibited by frictional materials, it is important to correctly incorporate them in the constitutive model, both in terms of their rate of development and their magnitude.

The primary goal of the present study is to screen, through a number of experiments, those features of sand behavior that can be considered "material parameters" and can be used for constitutive modeling of granular soils. Special attention is given of those features of material behavior that are related to dilatancy. For this purpose, a number of consolidated drained triaxial tests are performed under different stress conditions. Also a number of published experimental data are analyzed and useful trends of soil behavior are found.

## 2. SCOPE AND OBJECTIVES OF PRESENT STUDY

The objective of this study was to identify certain features of material behavior that can be used to aid in constitutive modelling of soils. Emphasis is given to dilatancy characteristics both before and after peak shear strength is obtained. The effects of confining pressure, initial density and stress path are both separately and collectively evaluated.

To carry out these objectives an experimental program was designed. The results of this program are combined with related existing literature to create solid information on soil behavior. The testing program includes a series of conventional triaxial compression test as well as two series of "unconventional" triaxial tests in which the confining pressure changes during the test. The purpose of the latter series is to investigate stress path dependency and to identify elastic and plastic trends in soil response.

All tests are carried out in two different densities. The relation of dilatancy, confining pressure, and density was thus evaluated.

### 3. REVIEW OF LITERATURE

#### 3.1 General:

Elasticity, viscosity and plasticity are three broad based material response phenomena upon which stress-strain laws are developed. Elastic materials are those whose relations between stress and strain are reversible. Linear elasticity applies when the relation is also linear. Viscous materials are those whose stress-strain relations involve time. For example, the strain response to an applied constant stress might increase over a period of time. Plasticity on the other hand, is a branch of the constitutive modeling theory which describes the time independent non-linear and inelastic behavior of materials. The accuracy of the constitutive model is highly dependent upon values of the material constants. Appropriate laboratory tests are required to obtain these material constants.

The earliest demonstration of volume changes accompanying shear deformation in sand was made by Reynolds in 1885, who showed experimentally that dense sands dilate when sheared. In 1936 Casagrande showed that whereas dense sands dilate during shear and exhibit a high angle of friction, loose sands compress during shear and develop a smaller angle of friction. He introduced the critical void ratio concept to describe the particular state of density at which a sand shears with no volume changes, and further demonstrated that the critical void ratio decreases as the confining pressure acting on the sand is increased.

In 1948 Taylor explained the influence of the void ratio on the angle of friction of a sand, and suggested that part of the shear stress required to cause failure of a dense sand is used in providing the energy required to permit the sand to expand against the confining pressure and that the shearing resistance is

therefore the combined result of two factors: friction and volume change component. Rowe (1962) concluded that throughout most of the range of void ratios there are three components of the strength of granular materials: (1) Strength mobilized by frictional resistance; (2) strength developed by energy required to rearrange and re-orient soil particles; and (3) strength developed by energy required to cause dilation of the material.

In a detailed analysis of the factors contributing to the strength of granular soils, Barden and Lee (1964) proposed that the energy required to cause dilation can be subdivided into (1) energy absorbed in friction as the mass dilates, and (2) energy required to do external work during volume changes.

Vesic and Barkdale (1963) presented the results of triaxial tests on a medium sand at confining pressures up to 10,000 psi and showed that (1) the Mohr envelope has a pronounced curvature up to pressure of about 50 Kg/cm<sup>2</sup> ; (2) the Mohr envelope for normal pressures ranging from 50 to 1600 Kg/cm<sup>2</sup> is essentially linear ; and (3) at confining pressures above about 20 Kg/cm<sup>2</sup> , shear deformations are accompanied by extensive crushing of the grains.

Lee et al. (1967) performed drained triaxial tests on samples of four initial densities. They found that an increasing confining pressure has three effects on dense sand: it reduces the brittle characteristics of the stress strain curve, it increases the strain to failure, and it decreases the tendency to dilate (Fig. 3.1). For loose sands they observed that at low pressures the tendency for dilation is not as strong as for dense sands, while at high pressures the tendency for compression is greater.

Vardoulakis et al. (1984) performed an extensive experimental study of the stress-strain behavior of dry sand in triaxial compression test. Emphasis was

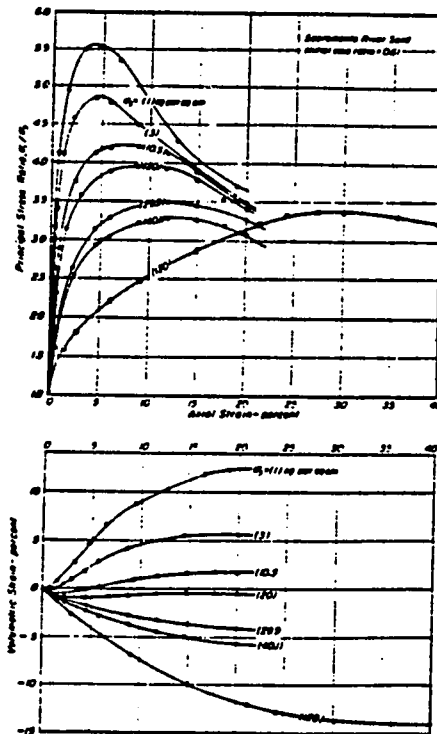


Fig.3.1 Stress-strain-volume change data for dense sand, after Lee(1967).

given on the behavior at small and large strains and rigid granular model of sand. According to the Hertz-Mindlin theory, the stress-strain behavior of a granular assembly is non linear even at very small strains, and the axial strain  $\epsilon_1$ , is approximated by a power law

$$\epsilon_1 = c \left[ \frac{\Delta\sigma_1}{\sigma_{10}} \right]^\alpha$$

Where  $\Delta\sigma_1 = \sigma_1 - \sigma_{10}$

$$\sigma_{10} = \sigma_2 = 400 \text{ KN per sq. meter}$$

The exponent  $\alpha$  is found to be constant for a given sand (Hettlers, 1981), with  $\alpha > 1$  when proportional loading is excluded. The factor  $c$  is found to depend on

the density and on the stress path, but not affected by the inter-granular pressure, as long as this pressure no longer exceeds a critical value  $p_{cr}$ . Another important property observed at small strains is that, starting from an isotropic stress state the incipient radial strain rate,  $\dot{\epsilon}_2 = 0$ . He also observed that very little softening occurs and dilation is at constant rate. This opposes Lee's findings who found intense softening accompanied by critical state. It is noted that Vardoulakis used lubricated ends and large sized sample which allowed for deformation uniformity even at large strains.

Varadarajan et al. (1987) performed a series of experiments to examine the effect of stress-path on the stress-strain-volume change relationships of a river sand. They concluded that these relationships are very much a function of stress-paths. Modulus values are evaluated for different stress-paths and relationships between stress-paths and modulus values are established.

### 3.2 Some fundamentals of plasticity Theory:

Since the aim of this work is to identify material parameters suitable for constitutive modeling it is considered appropriate to present here the basic principles behind the most important constitutive modeling approach for soils, namely the theory of plasticity. Four different facets are involved in the formation of a constitutive law based on the theory of plasticity:

- i) Yield criterion
- ii) Normality rule
- iii) Stress-elastic strain relationship
- iv) Evolution or hardening rule

### 3.2.1 Yield criterion:

The concept of a yield surface, yield criterion or yield function,  $F$ , is central to the plasticity theory. A material is said to yield at a point where a scalar condition, expressed as a function of stress, signifies initiation of irreversible response.

In the case of a material subjected to uniaxial state of stress, Fig.3.2, the yield function can be expressed as

$$F = \sigma - \sigma_y = 0 \quad (3.1)$$

Where  $\sigma$  is the present state of stress and  $\sigma_y$  is the stress level where initiation of yielding takes place. From Eqn. (3.1), if  $\sigma = \sigma_y$ ,  $F = 0$ , and the material is undergoing plastic strains. If  $\sigma < \sigma_y$ ,  $F < 0$ , the behavior is elastic.

For a multiaxial state of stress, nine components of stress are involved at a material point. So, construction of a yield function for a multi-axial state of stress should include all nine components of stress given by the stress tensor,  $\sigma_{ij}$ . Besides stresses, a yield expression may be a function of plastic work  $W^P$ ,

deformation (strain) history, which is usually expressed by  $\int \sqrt{d\epsilon_{ij}^P d\epsilon_{ij}^P}$ , and

other tensor or scalar valued internal variables. Therefore,  $F$  can be expressed as

$$F = F ( \sigma_{ij}, \epsilon_{ij}^P, W^P, \alpha_{ijk}, a_1, a_2 \dots a_N ) \quad (3.2)$$

$\alpha_{ijk}$  is a tensor valued internal variable and  $a_i$  ( $i = 1, 2, \dots, N$ ) are scalar valued internal variables.

If a material is assumed to be homogeneous, a yield function is valid everywhere in a material. Equation (3.2) can be expressed in terms of the principal stresses

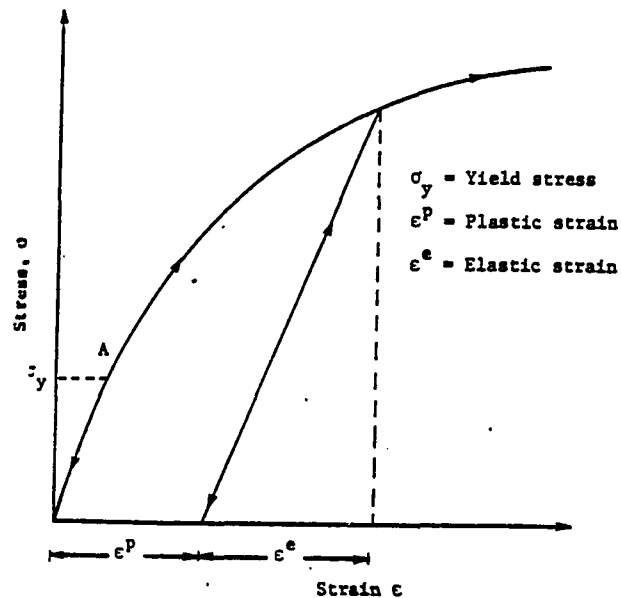


Fig.3.2 Typical uniaxial stress-strain response in Elasto plastic deformation.

and their directions; that is,

$$F = F ( \sigma_1, \sigma_2, \sigma_3, n_1, n_2, n_3, q ) = 0 \quad (3.3)$$

Where  $\sigma_1$ ,  $\sigma_2$  and  $\sigma_3$  are the principal stresses,  $n_1$ ,  $n_2$  and  $n_3$  are their direction cosines and  $q$  is a set of internal parameters. If we assume that the material is isotropic, then it does not have any preferred directions. Therefore, the yield criterion in Eqn. (3.3) can be expressed independent of directions; that is, for an isotropic material:

$$F = F ( \sigma_1, \sigma_2, \sigma_3, q ) = 0 \quad (3.4)$$

The principal stresses are physical quantities whose values do not depend on the co-ordinate system in which the components of stress were initially given. So

Eqn.(3.4) can be conveniently expressed in terms of the invariants of stress.

$$F = F ( J_1, J_2, J_3, q ) = 0 \quad (3.5)$$

where,  $J_1$ ,  $J_2$ , and  $J_3$  are the first, second and third stress invariants respectively, and are given by:

$$J_1 = \sigma_{ii}$$

$$J_2 = \frac{1}{2} \sigma_{ij} \sigma_{ji} \quad (3.6)$$

$$J_3 = \frac{1}{3} \sigma_{ij} \sigma_{jk} \sigma_{ki}$$

In the above expressions, as well as in the rest of this report, Einstein's tensor notation is used, with the index convention.

An initially isotropic material, during the process of plastic deformation, develops induced anisotropy. This is because plastic flow is directional. To include such induced anisotropy into the formulation, the approach of "kinematic hardening" is used, which allows for movement of the yield surface in the stress space.

### 3.2.2 Normality rule:

Normality rule, often called flow rule, defines the incremental plastic strains  $d\epsilon_{ij}^p$ .

In the theory of plasticity, incremental plastic strains are defined by assuming the existence of a function,  $Q$ , called the plastic potential. The directions of the plastic strain rates or increments are normal to  $Q$ . In other words, the increments of plastic strain,  $d\epsilon_{ij}^p$ , are proportional to the gradient of the plastic potential.

Introducing a constant of proportionality,  $d\lambda$ ,  $d\epsilon_{ij}^p$  can be expressed as (Hill,1950)

$$d\epsilon_{ij}^p = d\lambda \cdot \frac{\partial Q}{\partial \sigma_{ij}} \quad (3.7)$$

Where  $d\lambda \geq 0$

In the simplest case, the plastic potential and the yield function are the same. For strain hardening, the factor  $d\lambda$  in Eqn.(3.7) can be computed from the hardening rule. For perfectly plastic materials, it may be indeterminate, or it may be found from requirements of compatibility with elastic strains. In classical theory of plasticity, the yield function,  $F$ , and the plastic potential,  $Q$ , are assumed to be equal. The incremental plastic strain is then proportional to the gradient of  $F$ . This is called the "associative" law in plasticity. Description of material behavior based on the associative law has been found to be appropriate for a certain class of materials, especially those which are not pressure sensitive. For frictional materials, however, formulation of a constitutive relation based on the assumption that  $F = Q$  does not agree with observed behavior. This is predominantly reflected through excessive prediction of dilatant behavior.

### 3.2.3 Stress-Elastic Strain Relationship:

According to perfect plasticity when a material element is subjected to uniaxial tension or compression and reaches the plastic limit, it begins to deform under a constant state of stress: that is the plastic strain occurs without any increase of stress. Thus, at any point, the stress cannot be related to the total strain, but only to the elastic part of the total strain. Since for granular materials the stress-strain relations are nonlinear and inelastic, piecewise linearity is assumed and the incremental stress is related to the incremental elastic strain through the generalized Hooke's law.

$$d\sigma_{ij} = C_{ijkl} d\epsilon_{kl}^e \quad (3.8)$$

Where  $d\sigma_{ij}$  = stress increment,  $d\epsilon_{ij}^e$  = elastic part of the strain increment, and  $C_{ijkl}$  = elastic constitutive relation tensor.

A basic assumption made in the development of stress-strain relations for elastic-plastic materials is the decomposition of strains into elastic and plastic components:

$$d\epsilon_{ij} = d\epsilon_{ij}^e + d\epsilon_{ij}^p \quad (3.9)$$

Using Eqn. (3.8) and (3.9), the incremental stress  $d\sigma_{ij}$  can be expressed as

$$d\sigma_{ij} = C_{ijkl} \left[ d\epsilon_{ij} - d\epsilon_{ij}^p \right] \quad (3.10)$$

Eqn. (3.10) is the basis for explicit development of the stress-strain relations.

### 3.3 Evolution or hardening rule:

A material point is plastically stable if the stress at that point is a monotonic function of the strain (Fung, 1965). Except for the perfect plastic material, most materials exhibit increase of strength beyond the elastic limit. This phenomenon is called work or strain hardening. Hardening rules, which are also known as evolution rules, are intended to define the process of strength gain in a material due to permanent straining. Some materials also show loss in strength during the deformation process. This is called the strain-softening can be considered to be caused by disruption in the internal constitution of the material due to formation of discontinuities such as microcracks, fractures and voids. Hence, softening of material is due to structure or orientation of the small particles inside it.

### 3.3.1 Classifications of Hardening Rules:

In the theory of plasticity, there are three types of hardening rules:

- i) Isotropic hardening
- ii) Kinematic hardening
- iii) Anisotropic hardening

#### 3.3.1.1 Isotropic hardening:

In this hardening process, it is assumed that the yield surface expands uniformly about the center in the stress space. There are no rigid body rotation or translation of the yield surface. Fig.3.3 shows the hardening process for a

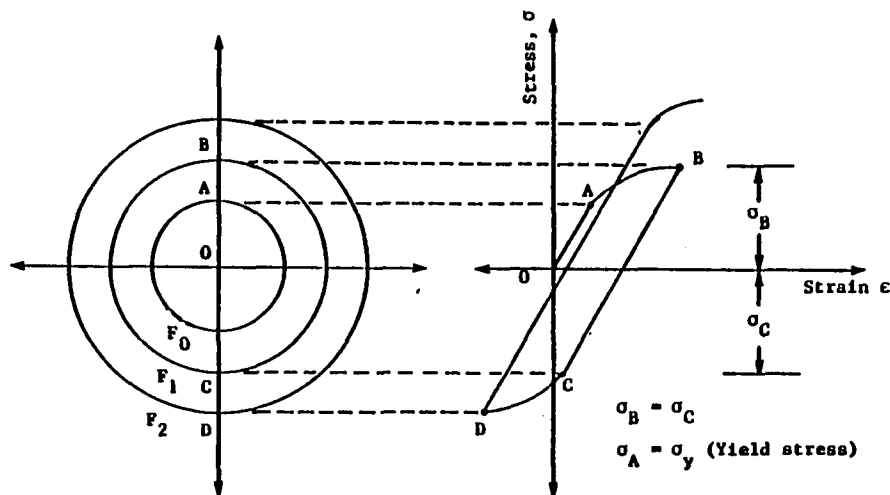


Fig. 3.3 Schematic of the Isotropic Hardening Rule for uniaxial stress-strain Response.

material subjected to a uniaxial state of stress.

The point A on the stress-strain curve represents the elastic limit. Any stress increment will not cause plastic strain unless the stress reaches the yield surface  $F_0$  corresponding to point A. Further application of stress will cause A to move to B, causing the yield surface  $F_0$  to expand uniformly to  $F_1$  about the origin O. Upon unloading from point B, and continued in the reverse direction, the material point behaves elastically until it reaches point C, such that  $|\sigma_B| = |\sigma_C|$ . From point C up to D, plastic deformation again sets in, and the yield surface expand to  $F_2$ . This continuous loading and unloading increases the elastic limit. A real material, however, starts yielding in the reverse loading before point C is reached. This phenomenon is known as the Bauchinger effect. However, for monotonic loading, isotropic hardening is adequate to describe material behavior.

#### 3.3.1.2 Kinematic Hardening:

Ishlinsky (1959) and Prager (1955, 1956) introduced the kinematic hardening rule. It is assumed that the yield surface translates in the stress space as a rigid body during the plastic deformation. Kinematic hardening rule predicts Bauchinger effect, but the yielding in the reverse loading may start too soon, which may not be the case with real materials.

#### 3.3.1.3 Anisotropic Hardening:

A yield surface can experience a combination of isotropic and kinematic hardening, which can be termed anisotropic hardening. Here, it is assumed that yield surface expands and translates simultaneously with the shape remaining the

same (Mroz, 1967). Anisotropic hardening rule is found to take the Bauehinger effect into account better than kinematic hardening rule.

## 4. TEST PROGRAM

### 4.1 General

Determination of the various material constants related to a constitutive model requires broad based, carefully conducted laboratory tests which include loading, unloading, and reloading. In this investigation, testing of materials is confined to Leighton Buzzard (LB) sand only. This is a subrounded, uniformly graded (U.S. sieve 20-30) material with a specific gravity of 2.65. The maximum and minimum void ratios are 0.81 and 0.53, respectively (Hashmi, 1986).

A number of consolidated drained tests are performed on saturated LB sand. These tests include Conventional Triaxial Compression tests (CTC), Constant Mean Pressure Triaxial Compression tests (CMPTC), Decreasing Mean Pressure Triaxial Compression tests (DMPTC) and Hydrostatic Compression (HC) tests. All tests are strain controlled, and are performed in a conventional triaxial testing device. Details on these tests are presented in subsequent sections of this thesis.

### 4.2 Description of Test Procedures:

Method of sample preparation: Samples for all tests are prepared using the so called "raining method" (Rad and Tumay, 1987). The details of the procedure used to prepare the sand samples are presented in the following.

1. A split mold (sample preparing cylinder fig.4.1 a ) with inside diameter equal to 1.4" and height 4.0"( which gives a soil sample of 1.4" in diameter and 2.8" in height ) is used to prepare the samples. The two halves of the mold are seperated. The entire instrument is cleaned and a small amount of vaseline is applied on the connecting faces of the cylinders. This minimizes the air leakage

in the mold when a vacuum is applied and allows easier manipulation of the membranes to help removing wrinkles. The halves are placed together and tightened using band clamp on the outer most edge of the cylinder.

2. A thin membrane is placed inside the mold and carefully stretched at both ends to minimize wrinkles.

3. Small vacuum (about 0.5 KPa) is applied and the membrane is pulled tightly on the inside face of the mold.

4. A porous stone and a filter paper are placed on top of the pedestal of the base of a triaxial testing device (fig 4.1 (b)). The mold is placed over the pedestal while maintaining the vacuum. A NGI triaxial machine is used for testing. Fig. 4.1 (b) shows the different parts of the testing device.

5. The sample is "rained" in the mold. For this purpose, a long tube on the top is used. The bottom of the tube is carefully placed over the top of the mold. The height of the cylinder controls the density of the resulting sample. In this study heights of 8' and 1' are used resulting to dense ( $e = 0.586$ ,  $D_r = 80\%$ ) and medium ( $e = 0.661$ ,  $D_r = 53\%$ ) samples respectively.

6. During the pouring of sand precaution is taken for allowing the air to escape from the mold. As the sand falls it achieve a consistent density throughout the sample. After the sand is completely rained out of the tube, the extra sand is slowly removed in thin layers by means of a smooth straight edge.

**Figure 1 - Sample Preparing Cylinder**

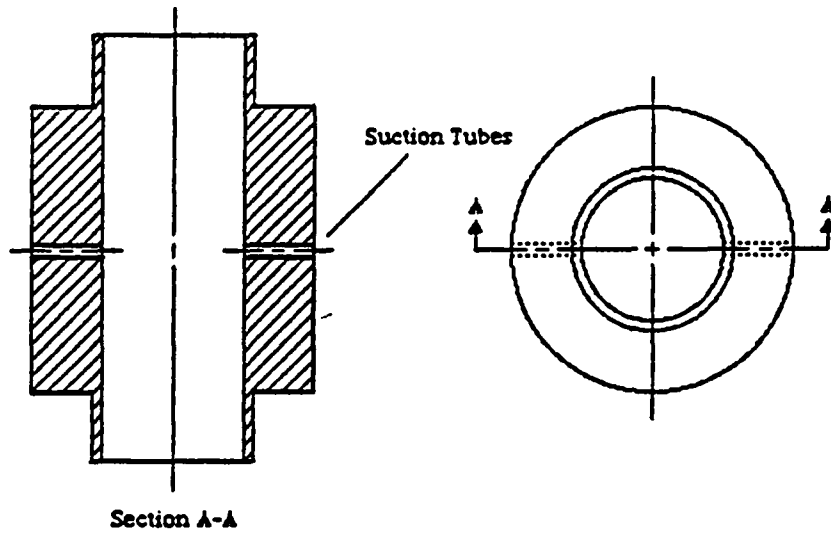


**Figure 2 - Membrane Expander**

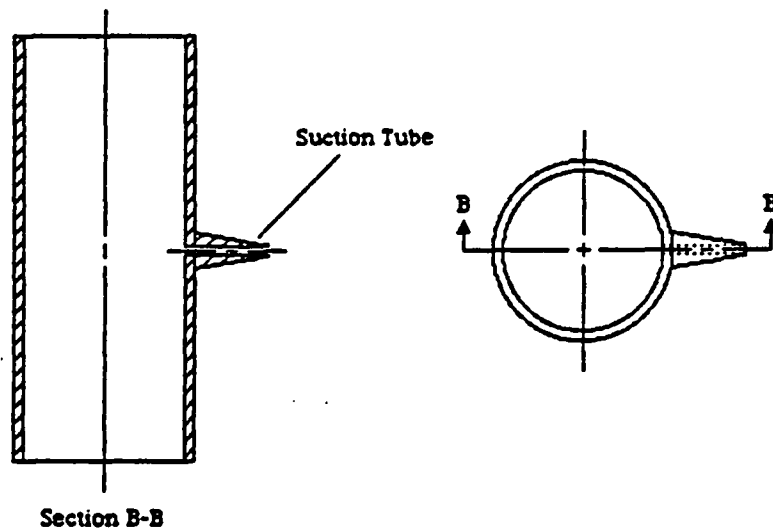


**Figure 4.1(a). Sample preparing Cylinder and Membrane expander.**

Schematic Diagram of the Triaxial Apparatus

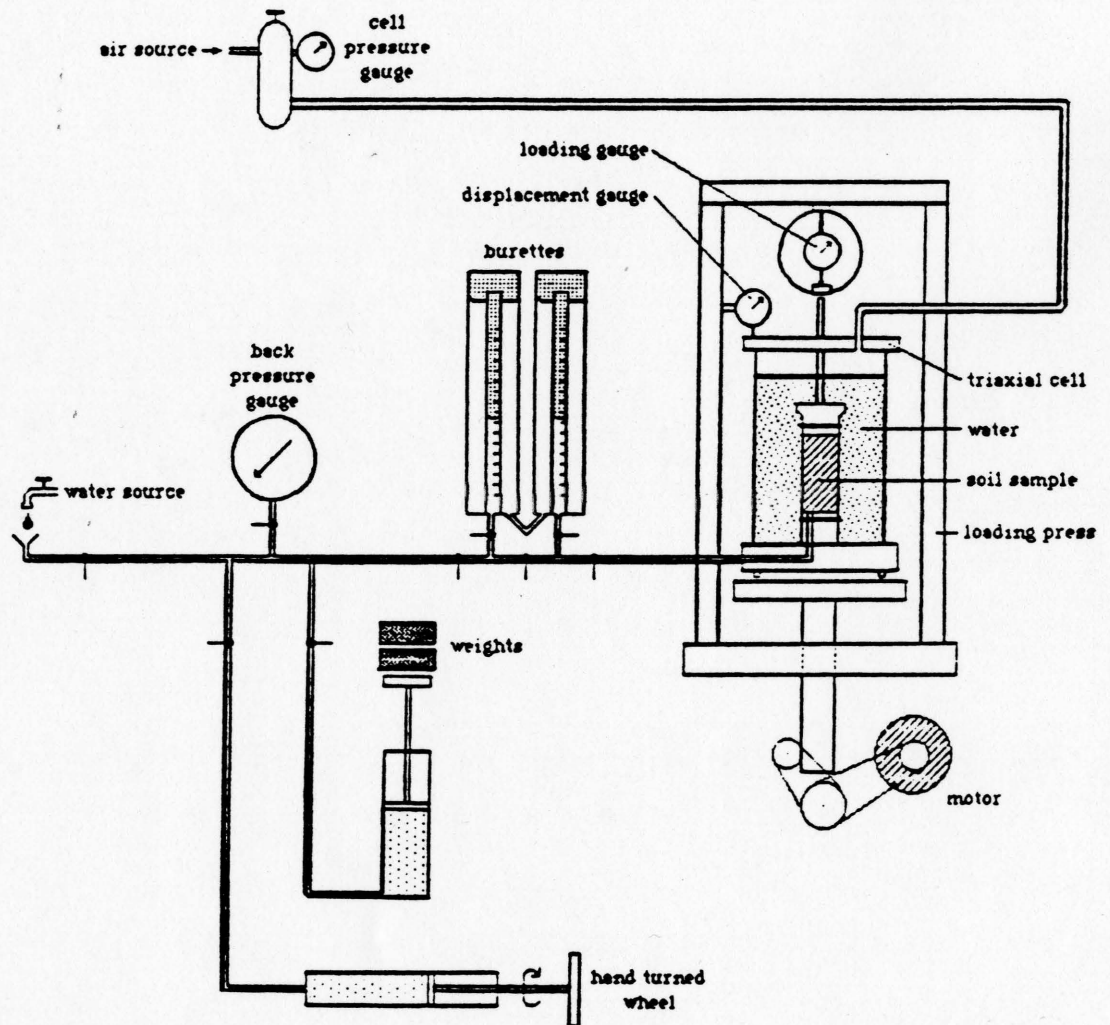


Figure 4.1 (b) Schematic Diagram of the Triaxial apparatus.

7. Another piece of filter paper followed by a porous stone is placed over the top of the mold. The loading cap is finally placed on top of the porous stone.

8. The prepared base plate is carefully placed on the loading table of the triaxial apparatus.

9. A vacuum of 1-2 kPa is applied to the sample to maintain its integrity.

10. The mold is removed carefully so that the sample is not disturbed. Another membrane is placed over the sample by membrane expander (fig.4.1) for extra protection from water leaks.

11. Two rubber o-rings are placed on each loading cap to prevent leakage.

12. While the vacuum is still applied to the sample, the top of the triaxial cell is lowered over the base plate and fasten tightly.

13. The triaxial cell is filled with water and a cell pressure of 50 kPa is applied gradually, while at the same time the vacuum is gradually removed.

14. In order to saturate the sample, water is allowed to flow under a head of 3 feet from the bottom drainage line to avoid any sample disturbance. This process is continued for about 24 hours until most air bubbles in the sample are displaced. At this stage the sample is nearly saturated.

15. To ensure full saturation, 300 kPa back pressure is applied. The cell pressure of course is always greater than the back pressure by 50 kPa.

16. At this point the sample is allowed to rest for few hours so that all air bubbles in the sample are dissolved. After this time, a slow flow is established and more water is allowed to flow through the sample, to remove the water with the dissolved air.

After the initial consolidation, the sample is "sheared" by applying deviatoric stress. In triaxial machine this is usually obtained by simply varying the vertical normal stress  $\sigma_1$  , while keeping constant or decreasing the cell pressure  $\sigma_3$  .

The steps followed for this procedure are described below.

1. A proving ring is attached to the top of the loading press.
2. A deflection micrometer is attached in vertical position to the side of the loading press.
3. Deviatoric stress is then applied to perform the shearing part of the triaxial test. In order to avoid excess water pressure build up, and facilitate the execution of the constant mean pressure, and reduced mean pressure tests, the relatively low strain rate of 0.683 mm per minute used.

### 4.3 Types of Consolidated, Drained Triaxial Tests:

The testing program includes four different drained triaxial tests. The test results are used to identify aspects of soil behavior which are important in the development of constitutive modeling of granular soils. Volume change and strength behavior under different confining pressures and initial densities are examined. Details of the tests performed in this study are presented in the following.

Conventional Triaxial Compression tests (CTC): This is the most commonly performed triaxial compression test, where the cell pressure is kept constant while the vertical stress is increased. The mean pressure increases as the vertical stress increases until the sample reaches failure. Typical stress paths for this test are presented in figure 4.2. Tests are performed under confining pressures of 100, 200, 300 and 400 kPa. These are all considered to be low confining pressures, for the densities used here.

Constant Mean Pressure Triaxial Compression tests(CMPTC): In this test, the vertical (major) principal stress is increased by  $\Delta\sigma$ , while the confining pressure is decreased by  $\Delta\sigma/2$ . This procedure results to constant mean pressure throughout the test. Typical stress paths for this test are presented in figure 4.2. The tests that were conducted in this study maintained mean pressures of 100, 200 and 300 kPa.

Decreasing Mean Pressure Triaxial Compression tests(DMPTC): In this test

increase of the vertical (major) principal stress by  $\Delta\sigma$  is accompanied by decrease of the confining pressure by  $\Delta\sigma/3$  . This results to a decrease of mean pressure with constant rate until the sample reaches failure. Typical stress path of this test are shown in figure 4.2. Tests were performed under initial mean pressures of 100, 200 and 300 kPa.

Hydrostatic Compression test (HC): This is an isotropic consolidation test aimed to produce information of the volumetric behavior of the material due to compression only.

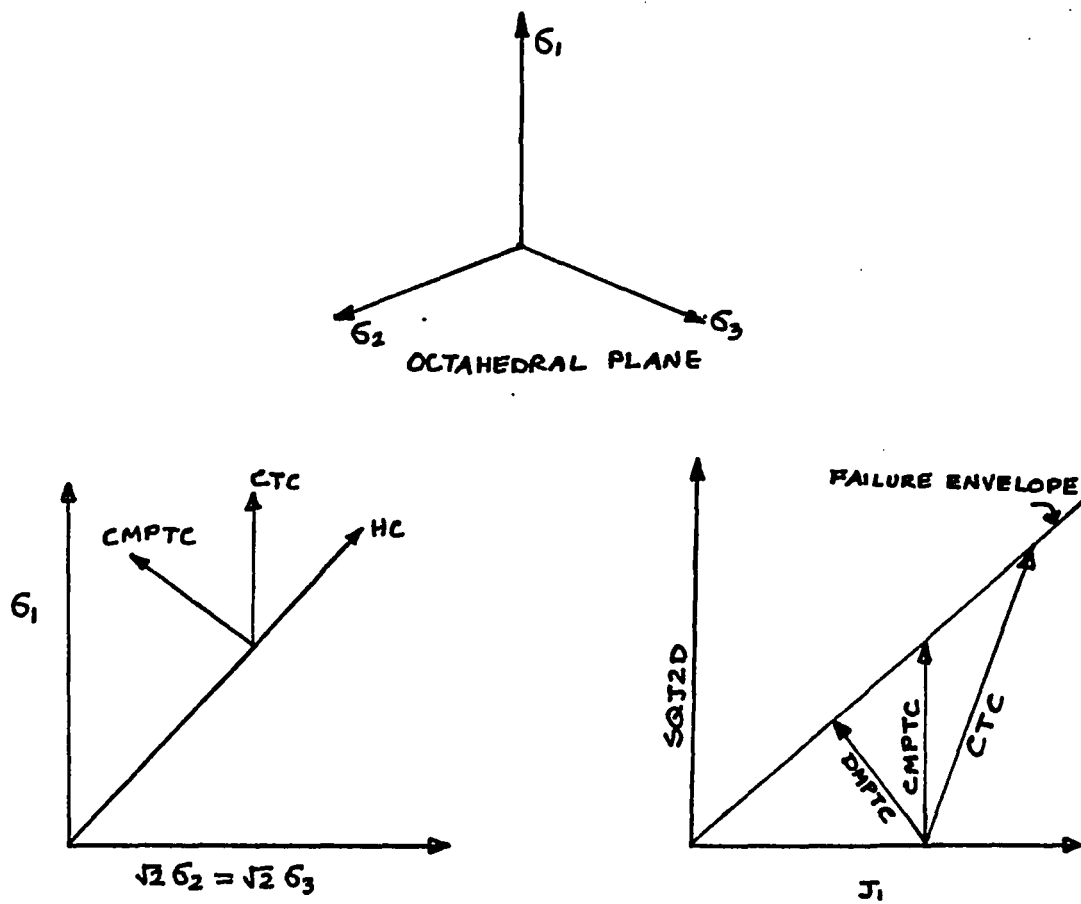


Fig.4.2 Different stress-paths.

#### 4.4 RESULTS OF TESTS:

We intend to investigate the effects of different parameters on shear and volumetric behavior of granular soils. In general, as confining pressure increases, strength increases, while as shear increases, the slope of stress-strain decreases, i.e. the material approaches failure. All acceptable constitutive models of soils are capable of handling these general features of soil behavior. However, the success in accurately describing soil behavior is limited. Investigators seem to disagree on the choice of significant material parameters. This is partly because parameters that seem to be important in some studies, prove to be completely unimportant in others. Some investigators for example find that sands reach a critical state of stress, i.e zero volumetric strain rate (Lee, 1970) while others find that sands dilate under a constant rate for the "useful" and accurately measured range of deformations (Vardoulakis, 1984). This phenomenon and the significance of the observations are discussed later in the chapter. Also, a number of researchers have found that many soils soften ( in simple terms they exhibit negative slope of the stress-strain behavior). The interpretation of this phenomenon and the validity of these observations have not been under universal agreement by all researchers. In the following, we make a brief presentation of the symbols and nomenclature that is used in here to present and interpret the results observed in this study. Keeping the classical soil mechanics conventions, we define compressive normal, stresses and strains to be positive. For volumetric changes, dilation is taken as positive. Only effective stress measures are considered here. During hydrostatic states of stress, the confining pressure is expressed as

$$\sigma_c = \sigma_1 = \sigma_2 = \sigma_3$$

For general loading condition, stresses are generally expressed in terms of invariant stress quantities such as the first stress invariant  $J_1$ , and the second invariant of the deviatoric stress  $J_{2D}$ .

The first stress invariant  $J_1$  is defined as

$$J_1 = \sigma_1 + \sigma_2 + \sigma_3 \quad (1)$$

The second deviatoric stress invariant is given by

$$J_{2D} = \frac{1}{2} S_{ij} S_{ij} \quad (2)$$

(repeated indices imply summation according to Einstein convention), where  $S_{ij}$  is the deviatoric stress given by

$$S_{ij} = \sigma_{ij} - \frac{1}{3} \delta_{ij} \sigma_{kk}$$

$\delta_{ij}$  is Kronecker's delta and is equal to 1 if  $i = j$  or 0 otherwise.  $J_{2D}$  can be written in terms of principal stresses as

$$J_{2D} = \frac{1}{6} \left[ (\sigma_1 - \sigma_2)^2 + (\sigma_2 - \sigma_3)^2 + (\sigma_3 - \sigma_1)^2 \right]$$

which for the triaxial test with horizontal stress isotropy becomes

$$J_{2D} = \frac{1}{3} (\sigma_1 - \sigma_3)^2$$

The square root of  $J_{2D}$  provides a good measure of generalized shear stress, and for this reason it is a very useful quantity in the constitutive modeling of materials. In a similar manner, the strains are expressed by invariant quantities such as the first invariant of strain  $I_1$  and the second invariant of deviatoric

strain  $I_{2D}$  given by

$$I_1 = \frac{\Delta V}{V_0} = \epsilon_{ii} = \epsilon_1 + \epsilon_2 + \epsilon_3$$

$$I_{2D} = \frac{1}{2} e_{ij} e_{ij}$$

Where  $\epsilon_1 = \epsilon_z$  is the vertical axial strain,

$\epsilon_2 = \epsilon_r$  is the radial strains

$\epsilon_3 = \epsilon_\theta$  is the tangential strains and

$$e_{ij} = \epsilon_{ij} - \frac{1}{3} \delta_{ij} \epsilon_{kk}$$

In terms of principal strains,

$$I_{2D} = \frac{1}{6} [(\epsilon_1 - \epsilon_2)^2 + (\epsilon_2 - \epsilon_3)^2 + (\epsilon_3 - \epsilon_1)^2]$$

which for the triaxial test, assuming isotropic response, becomes

$$I_{2D} = \frac{1}{3} (\epsilon_1 - \epsilon_3)^2$$

The square root of  $I_{2D}$  provides a good measure of generalized shear strain on a medium and for this reason, combined with  $\sqrt{J_{2D}}$ , provides a useful means of describing general shear stress-strain response. In the following, the stress-strain and volumetric response curves of Leighton Buzzard sand, are described.

Fig.4.3 a & b shows results from hydrostatic compression (HC) test. It is observed that both the loading and unloading curves are highly nonlinear. Also, the upward trend of the stress-strain curve with increase of confining pressure suggests that the material stiffens under pure hydrostatic state of stress. This behavior has also been observed by other researchers (Lee and Seed, 1967,

Hashmi 1986, Lade 1987, and Varadarajan 1987). Shear stress-strain relations in terms of the second deviatoric invariants are presented in fig.4.4, 4.5 and 4.6 for three types of consolidated drained test ( CTC, CMPTC & DMPTC) for dense ( $D_r = 80\%$ ) and loose ( $D_r = 53\%$ ) sand. Each figure shows the effect of different confining pressures and relative densities. As expected, sand becomes stronger with the initial confining pressures. Also, sand tested at a lower initial density but with the same confining pressure exhibits lower ultimate strength than that of higher initial density.

The relations presented in figure 4.4 is replotted in figure 4.7 using normalized shear stresses. The normalization is obtained by dividing  $\sqrt{J_{2D}}$  by the initial confining pressure  $\sigma_3$ . We observe that the material exhibits stiffer behavior at lower confining pressure.( i.e. the failure envelop shows a slight curvature for larger confining pressure.)

Volumetric versus shear strains for loose and dense sands in terms of  $I_1$  vs.  $\sqrt{I_{2D}}$  for three tests (CTC, CMPTC and DMPTC) are plotted on figure 4.8 through 4.13. It is found that in CTC tests sand compresses initially and then dilates with the increase in shear strains. This is observed for both dense and loose sand samples. However, it is also observed that dilation takes place sooner for denser samples and for smaller confining pressures. Dilation continues at a steady rate beyond peak failure. Dilation angle for CTC test decreases slightly

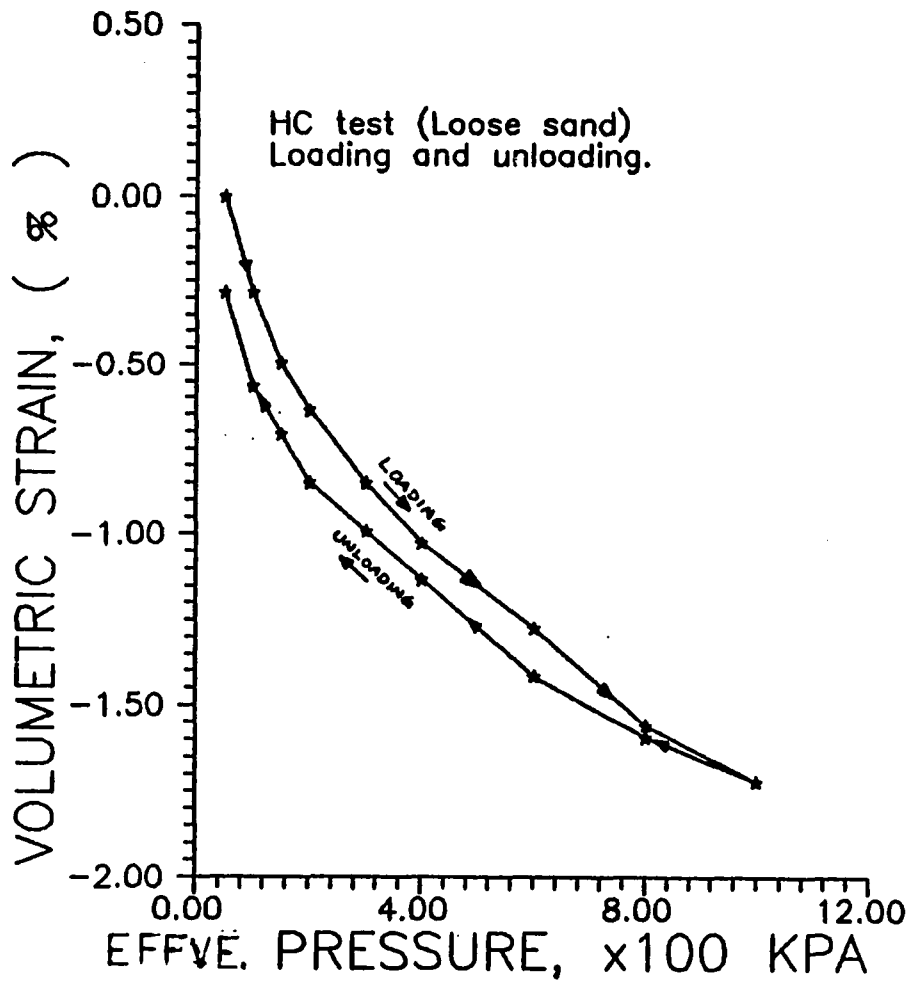


Figure 4.3 (a) Plot of Effective Pressure vs. Volumetric strain for HC Test on Loose LB Sand.

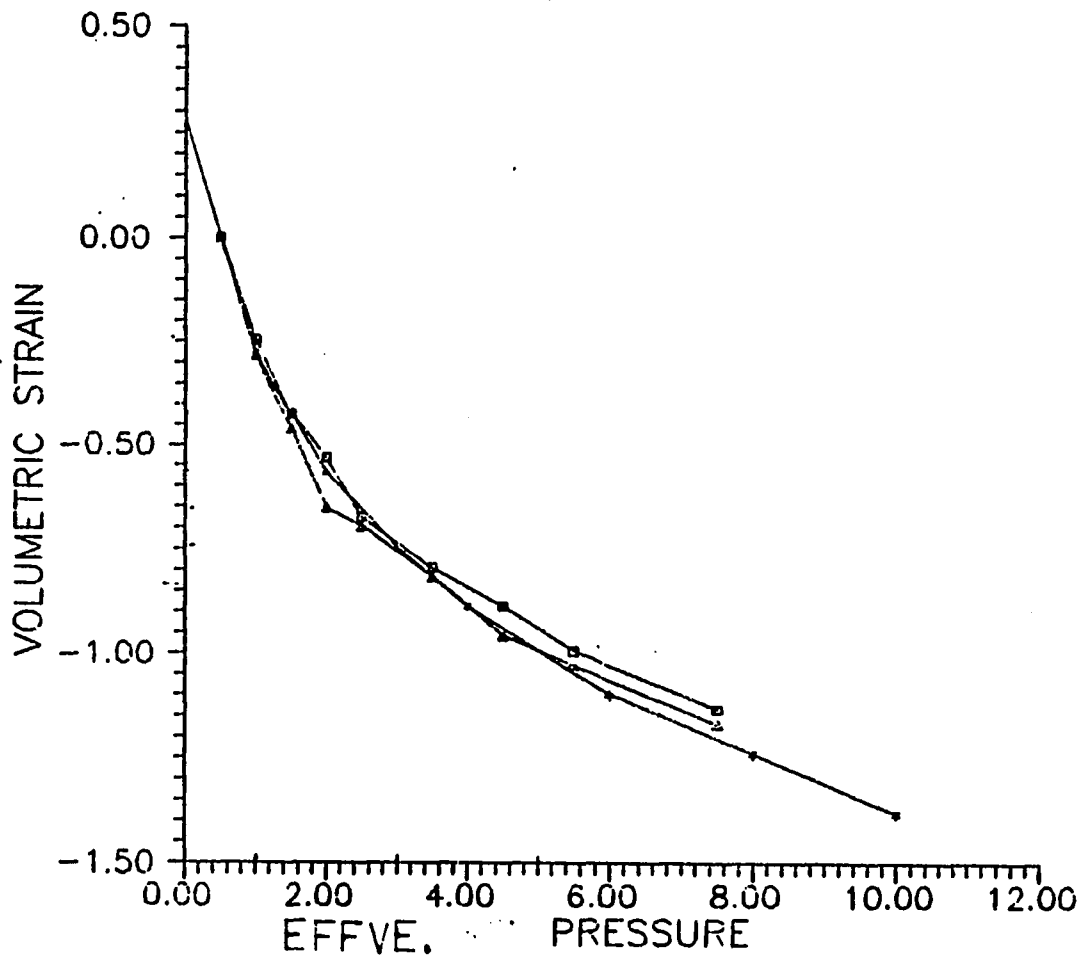


Figure 4.3 (b) Plot of Effective Pressure vs. Volumetric strain for HC Test on Dense LB Sand.

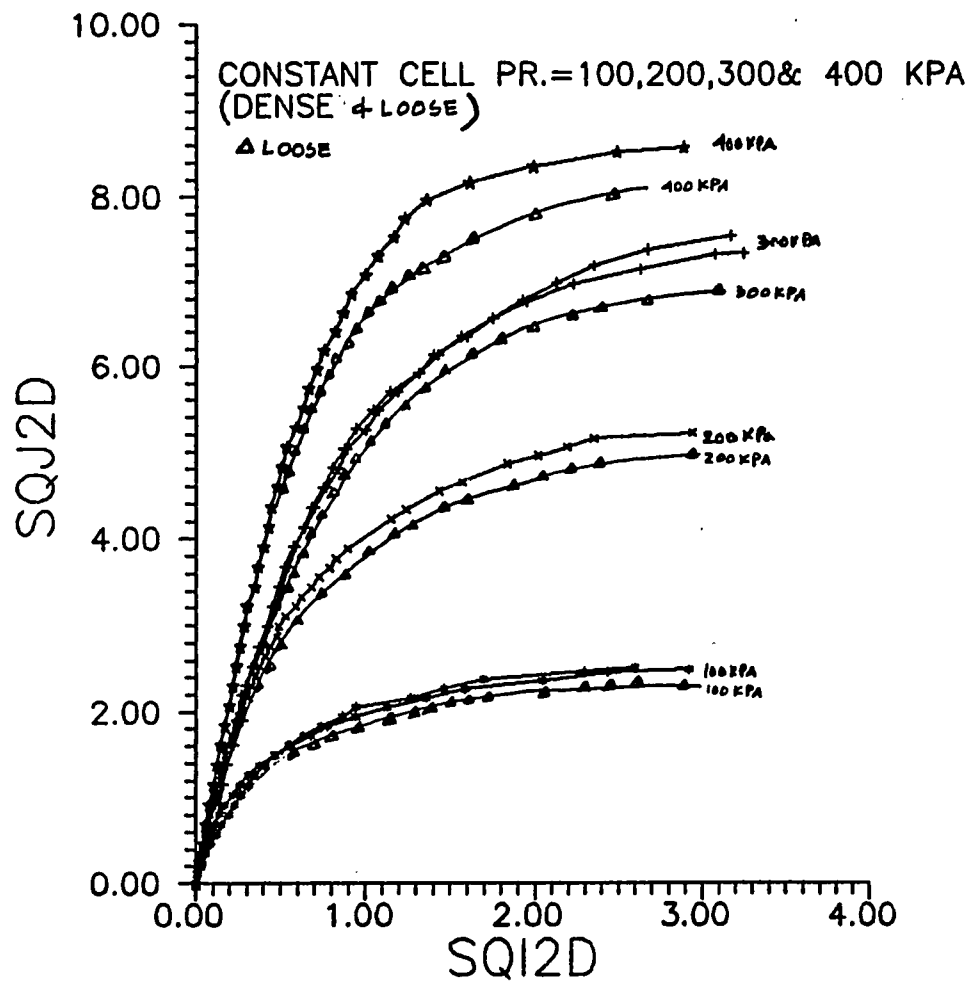


Figure 4.4. Shear stress-strain relations in terms of the second deviatoric invariant of CTC Test on LB Sand (Loose and Dense).

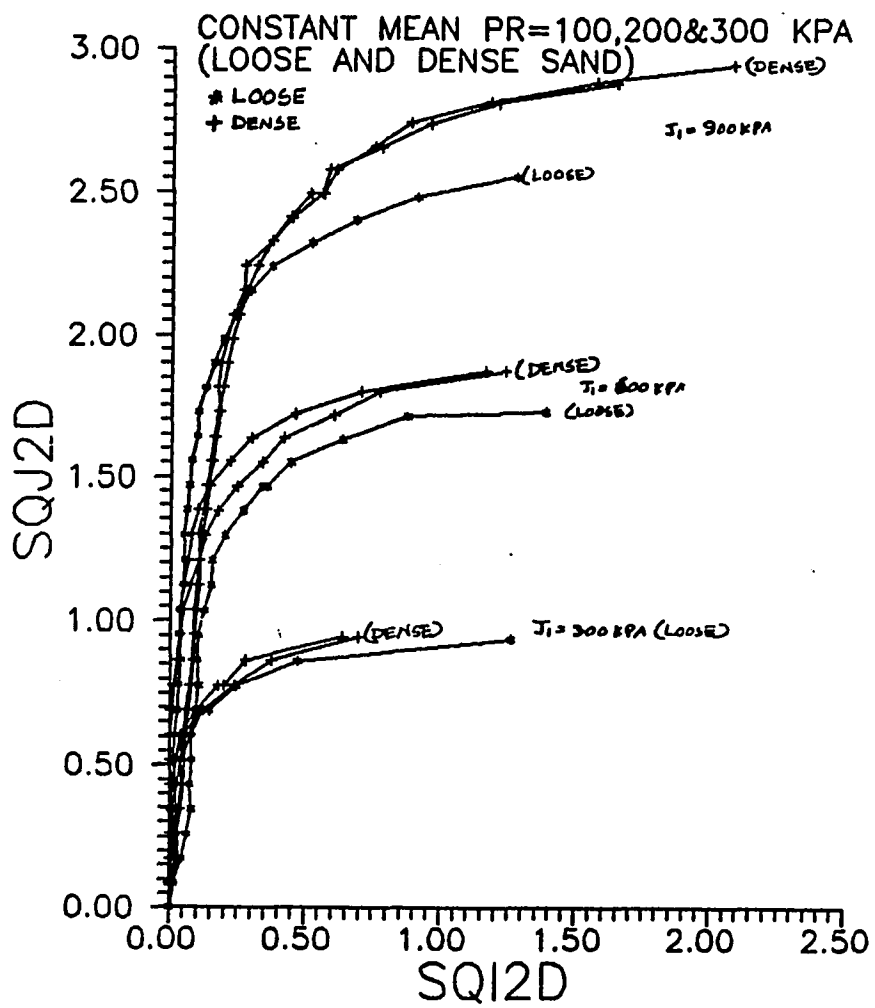


Figure 4.5. Shear stress-strain relations in terms of the second deviatoric invariant of CMPTC Test on LB Sand (Loose and Dense).

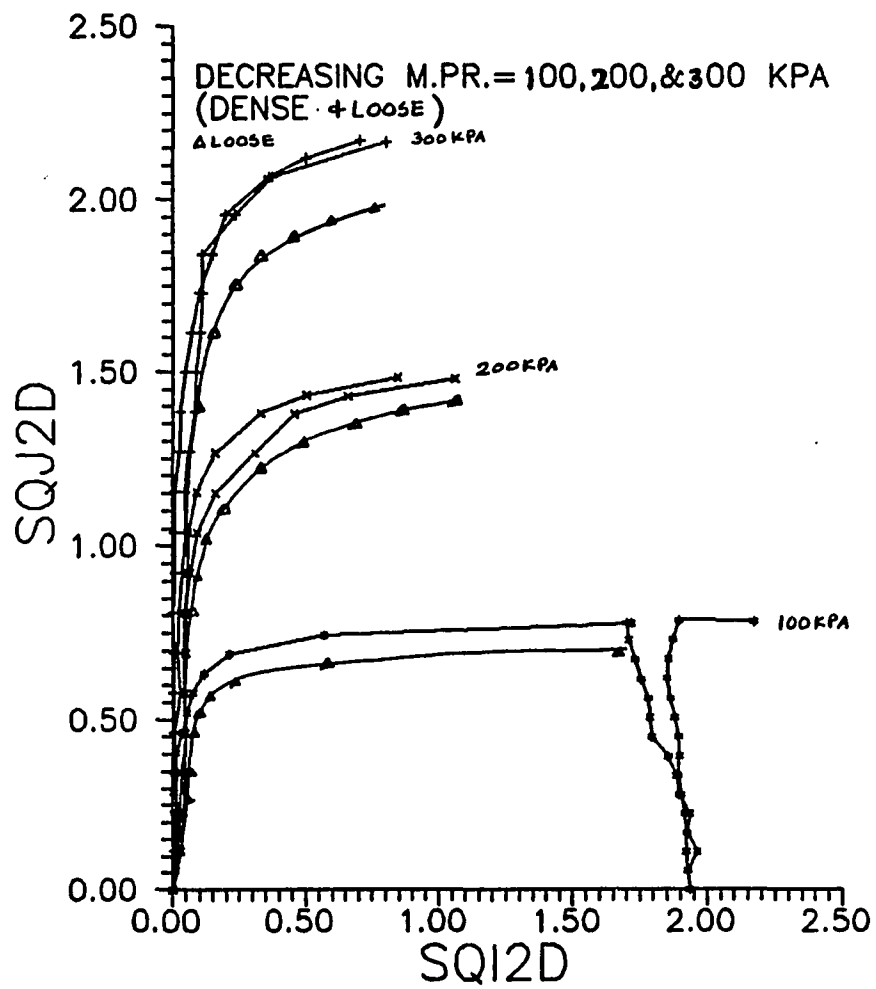


Figure 4.6. Shear stress-strain relations in terms of the second deviatoric invariant of DMPTC Test on LB Sand (Loose and Dense).

with confining pressure. Test results from CMPTC and DMPTC tests show different behavior from CTC tests (fig.4.9, 4.10, 4.12 and 4.13). In these tests, sand dilates from the beginning of shearing. Comparison of CTC tests with CMPTC and DMPTC tests suggests that the initial volume compression observed in CTC tests is predominantly due to the increase of mean pressure. To test this assumption, the results of a hydrostatic compression tests are superposed on both the CTC test and DMPTC test by using volumetric changes from HC tests. It is found that in both cases the resulting curves are almost identical to the ones of CMPTC tests. For small deformations, the volumetric curves of CTC and DMPTC tests collapse on the CMPTC test curve (fig 4.14 through 4.25).

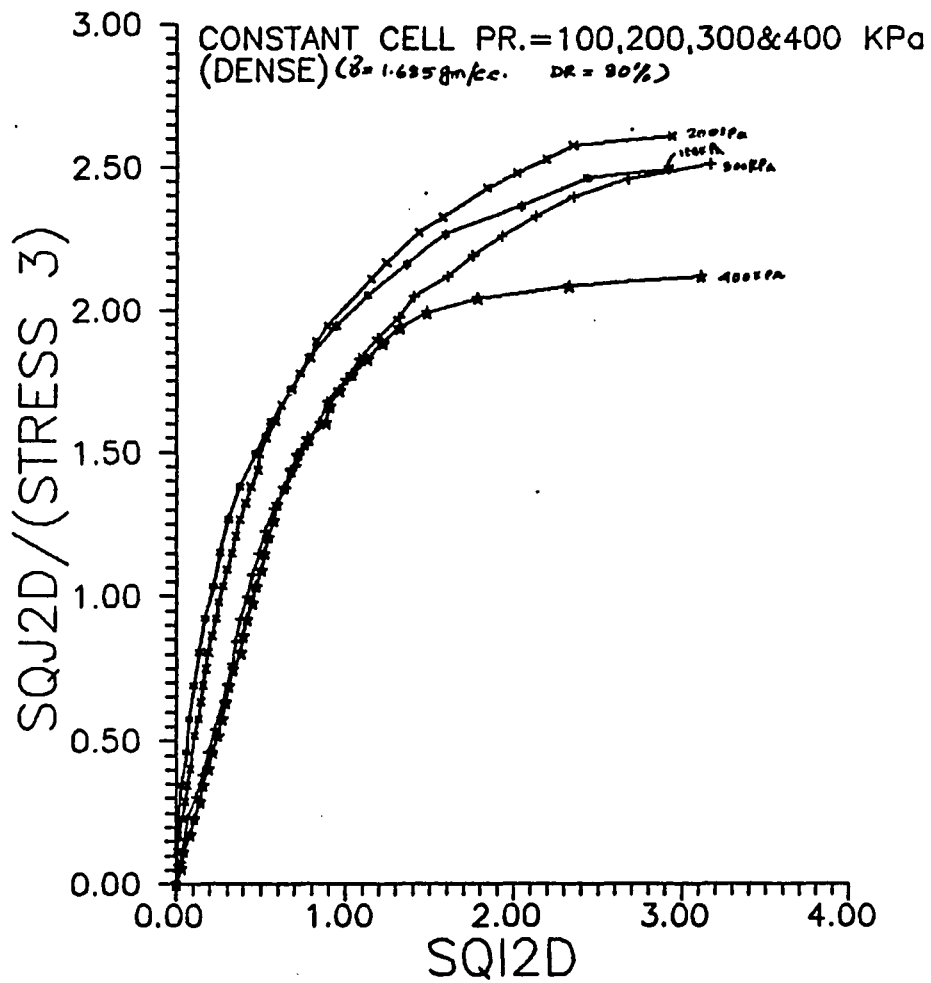


Figure. 4.7. Plot of Normalized shear stress vs. second strain invariant for CTC Test on LB Sand.

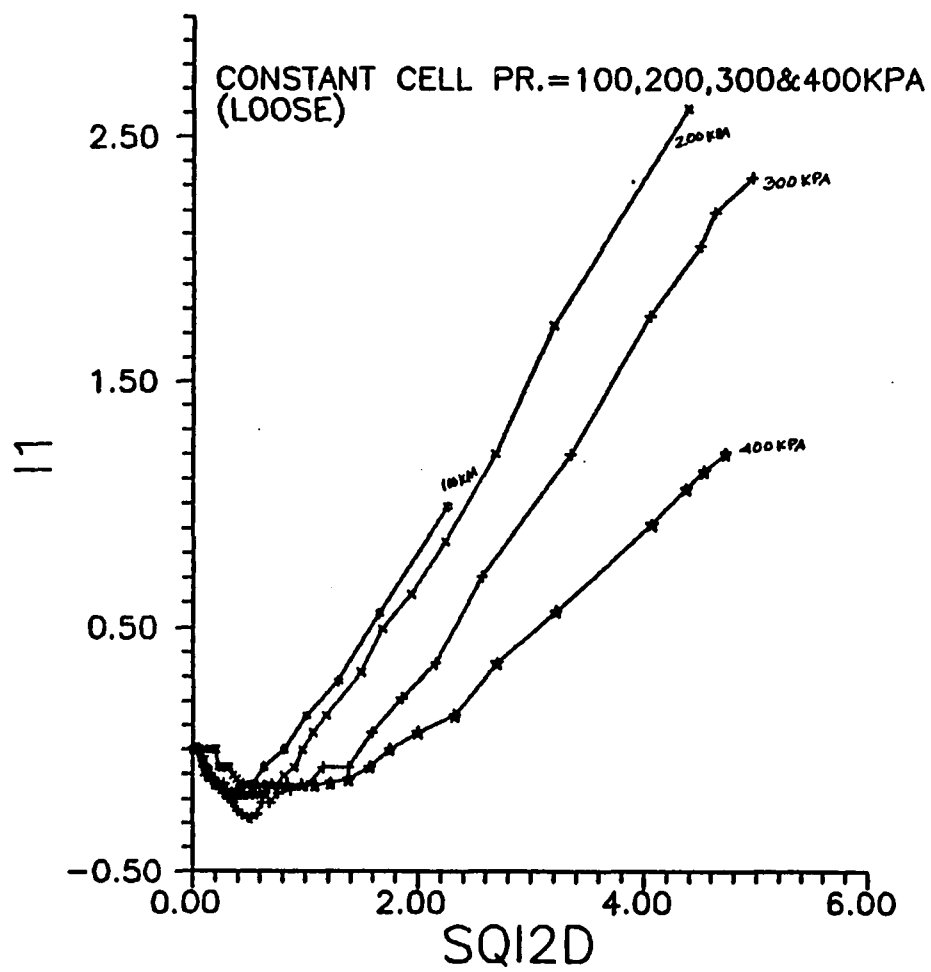


Figure. 4.8. Volumetric response in terms of the second deviatoric invariant of CTC Test on LB Sand (Loose).

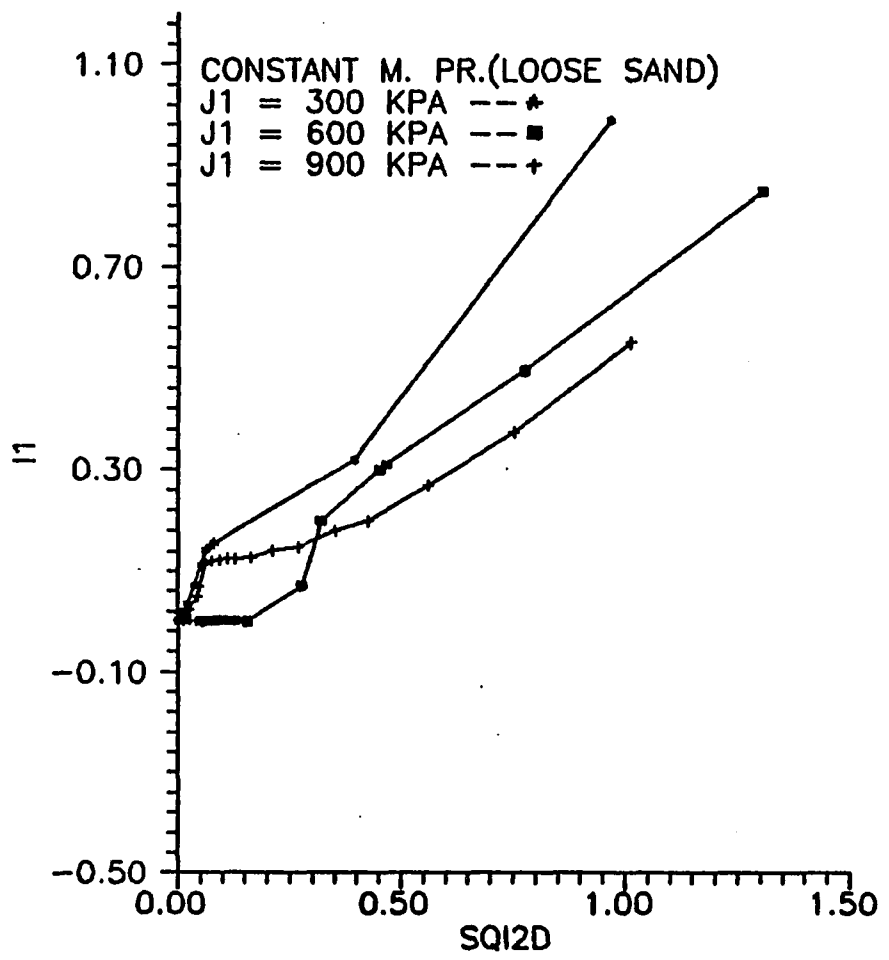


Figure. 4.9. Volumetric response in terms of second deviatoric invariant of CMPTC Test on LB Sand (Loose).

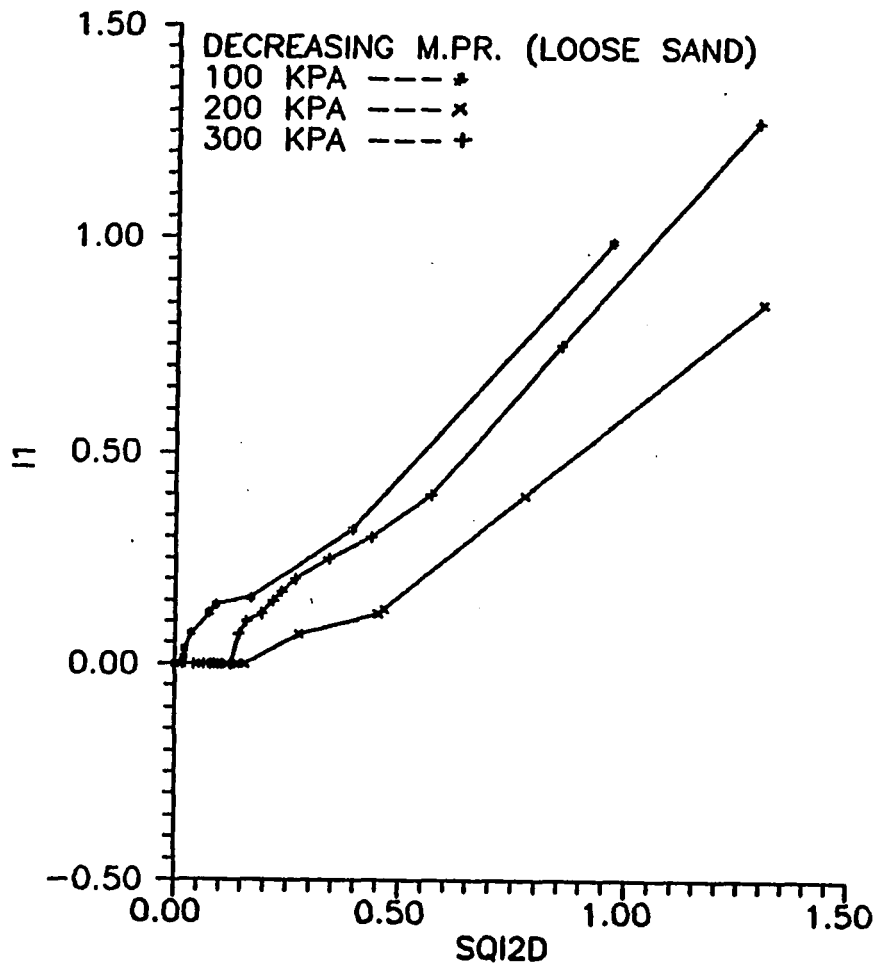


Figure 4.10. Volumetric response in terms of second deviatoric invariant of DMPTC Test on LB Sand (Loose).

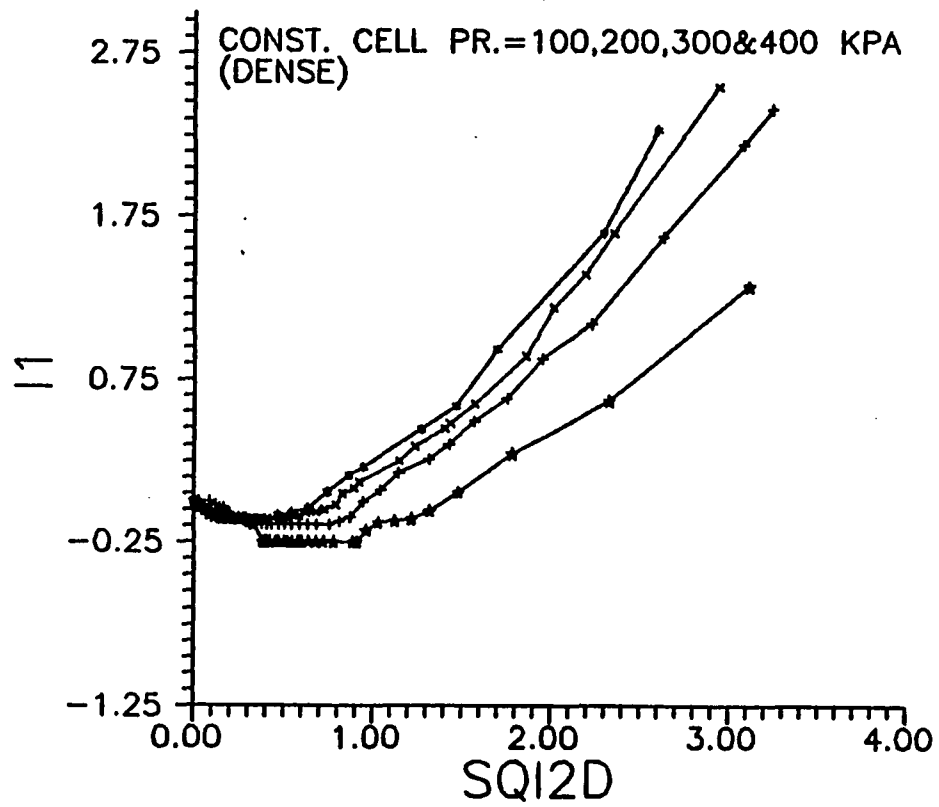


Figure 4.11. Volumetric response in terms of second deviatoric invariant of CTC  
Test on LB Sand (Dense).

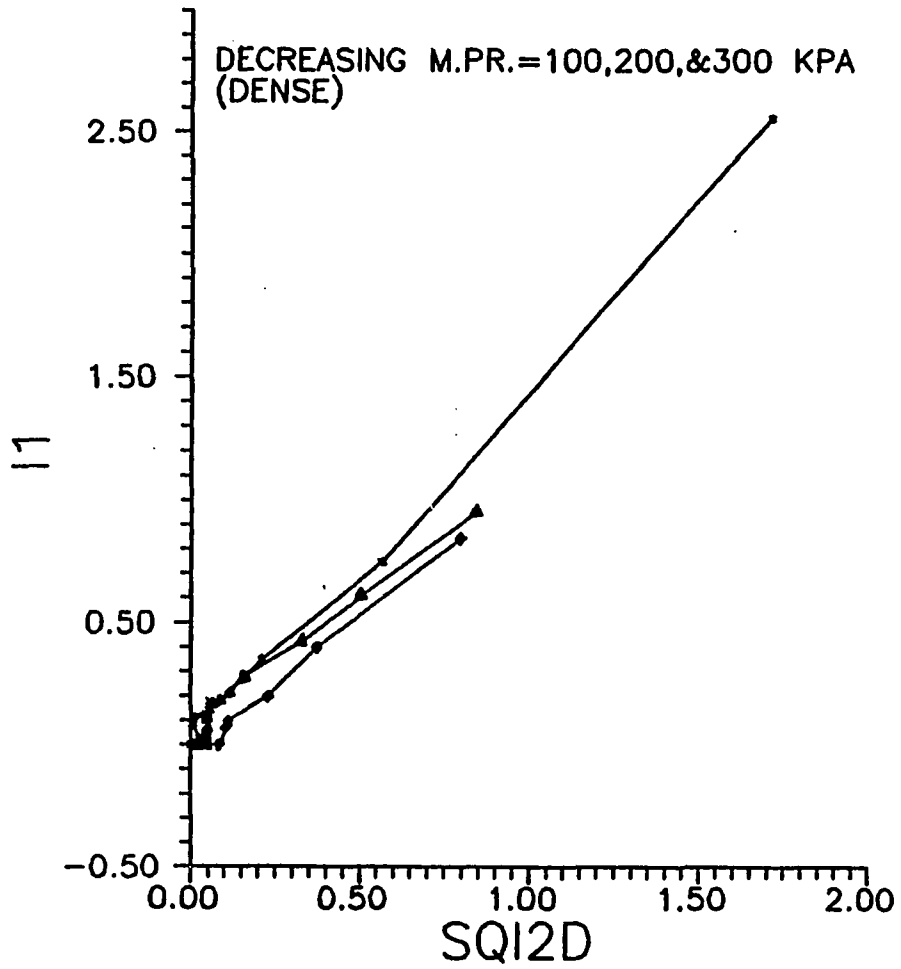


Figure 4.12. Volumetric response in terms of second deviatoric invariant of DMPTC Test on LB Sand (Dense).

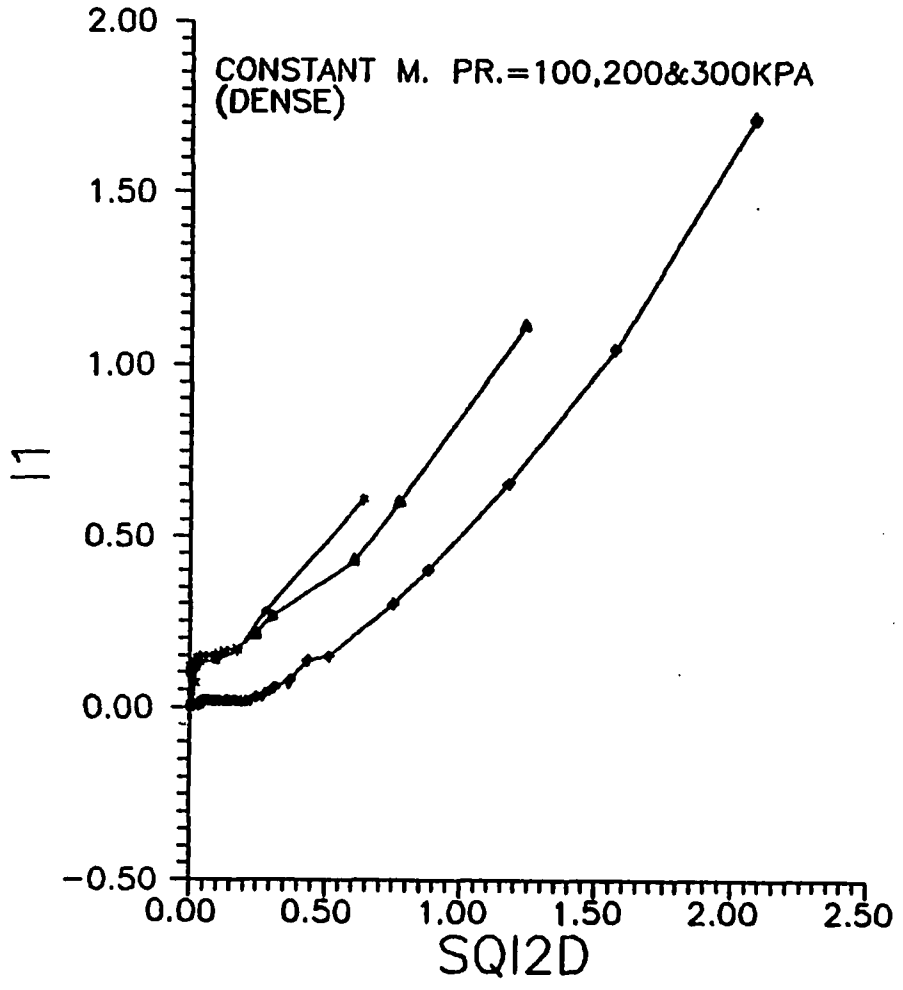


Figure 4.13. Volumetric response in terms of second deviatoric invariant of CMPTC Test on LB Sand (Dense).

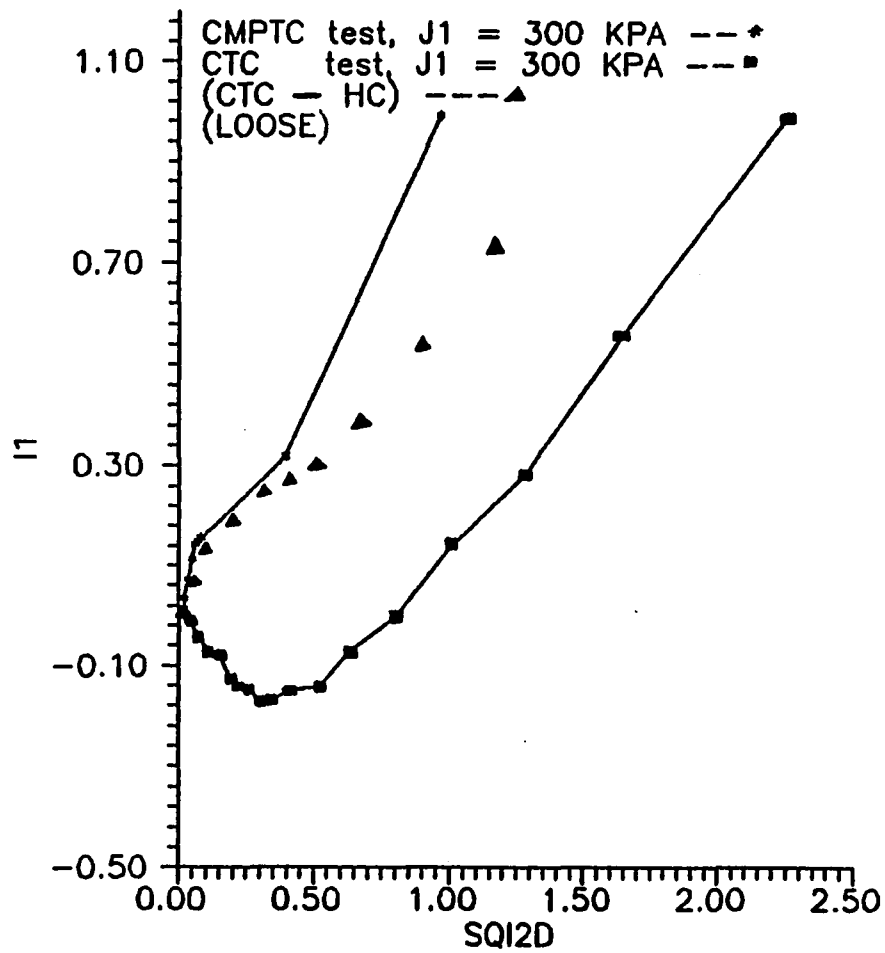


Figure 4.14. Comparison of Volumetric responses between CMPTC and CTC Test on LB Sand,  $J_1 = 300$  KPa (Loose).

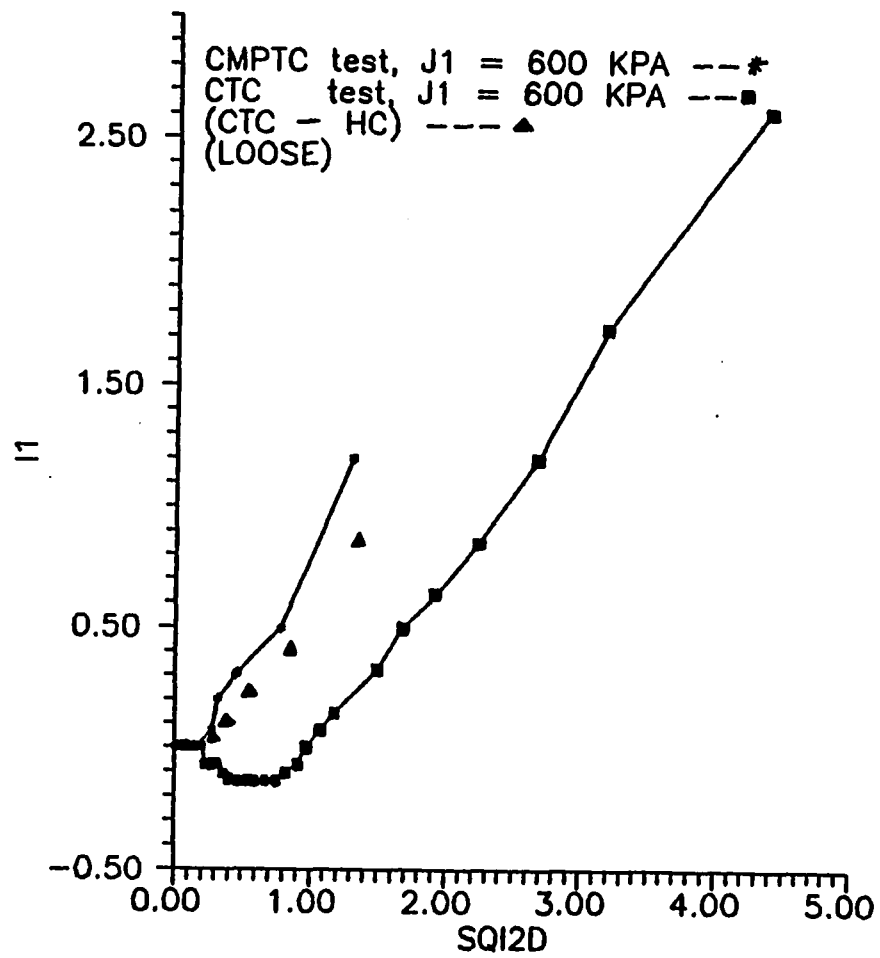


Figure 4.15. Comparison of Volumetric responses between CMPTC and CTC  
 Test on LB Sand,  $J_1 = 600$  KPa (Loose).

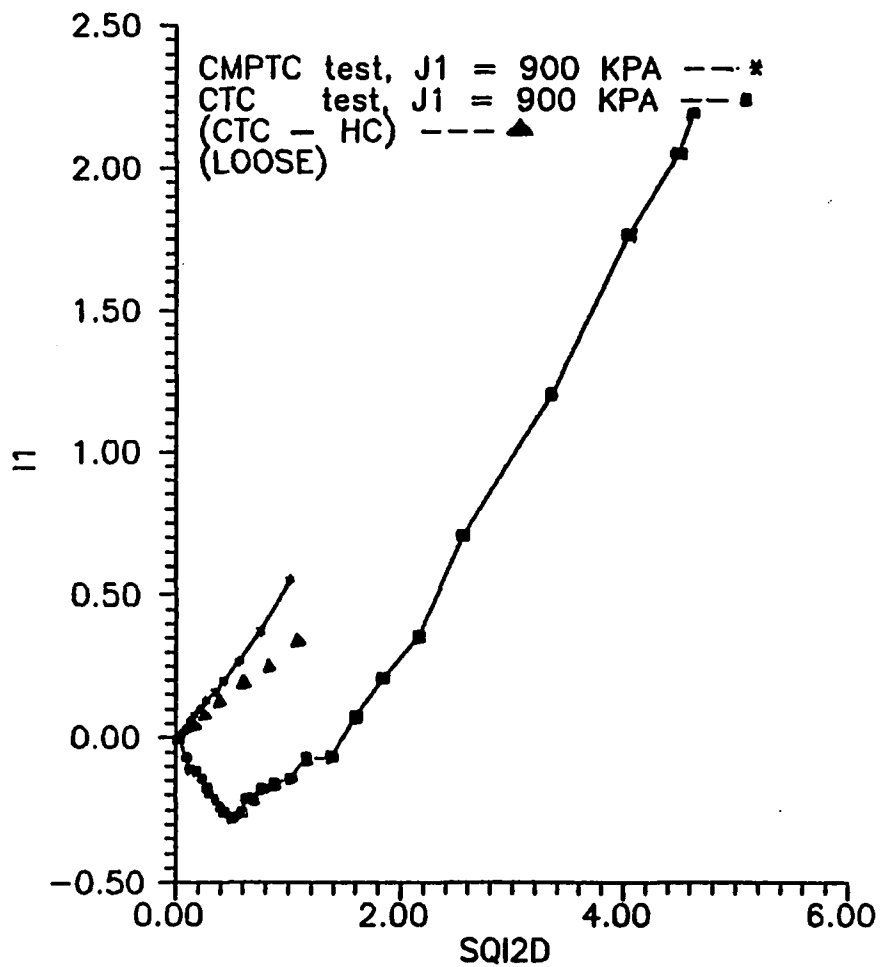


Figure 4.16. Comparison of Volumetric response between CMPTC and CTC  
 Test on LB Sand,  $J_1 = 900$  KPa (Loose).

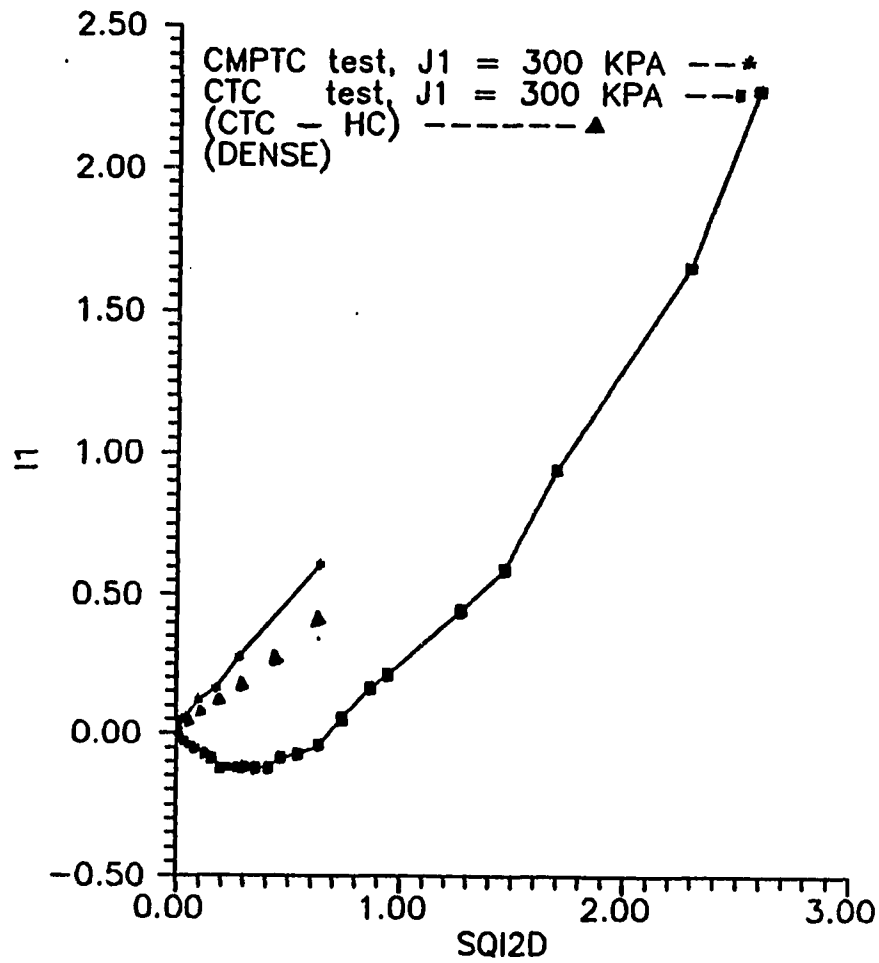


Figure 4.17. Comparison of Volumetric response between CMPTC and CTC Test on LB Sand,  $J_1 = 300$  KPa (Dense).

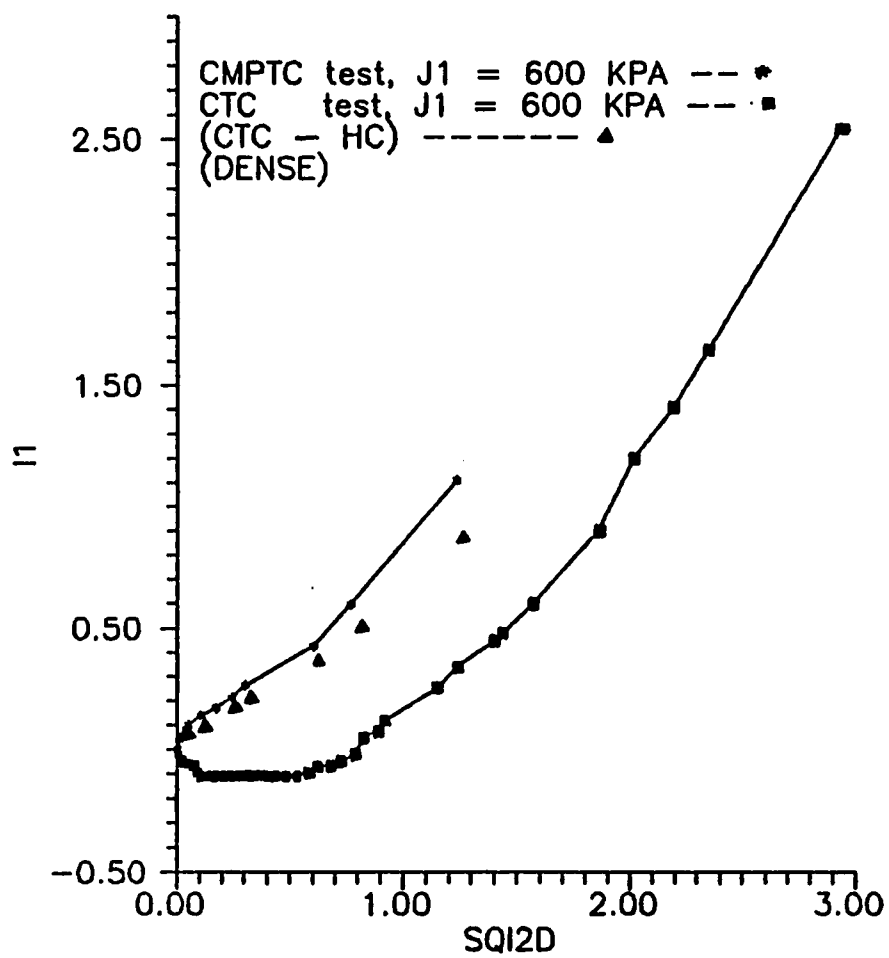


Figure 4.18. Comparison of Volumetric response between CMPTC and CTC Test on LB Sand,  $J_1 = 600$  KPa (Dense).

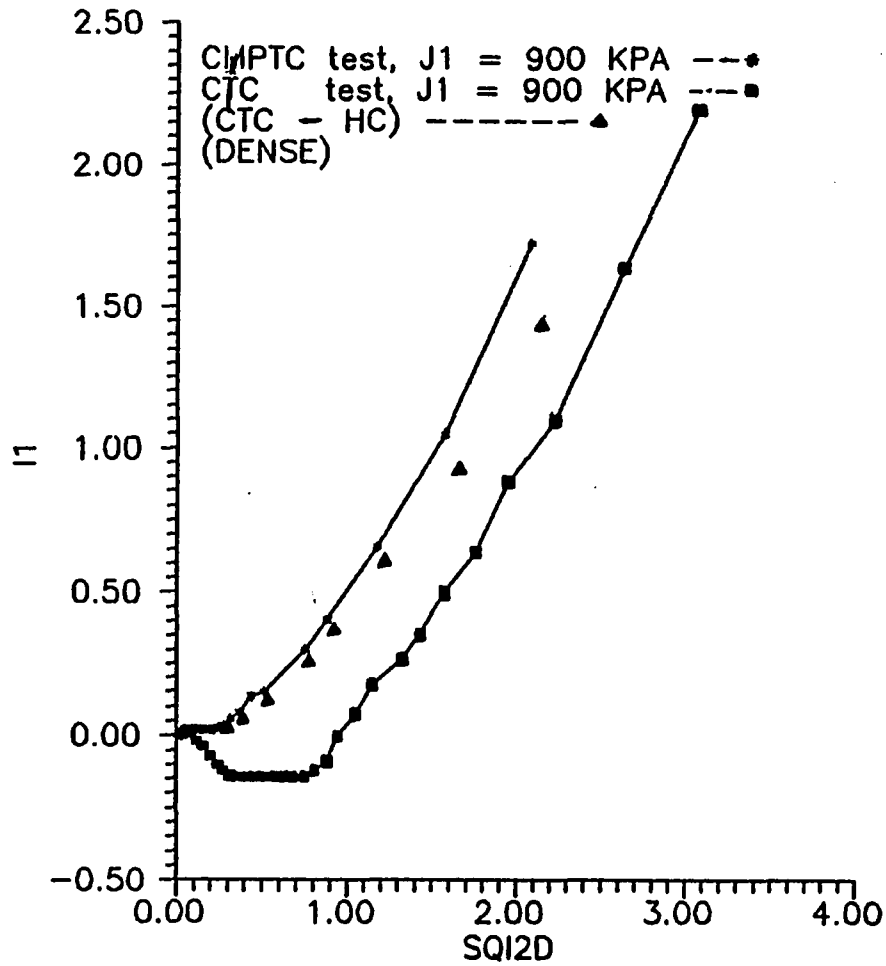


Figure 4.19. Comparison of Volumetric response between CMPTC and CTC Test on LB Sand,  $J_1 = 900$  KPa (Dense).

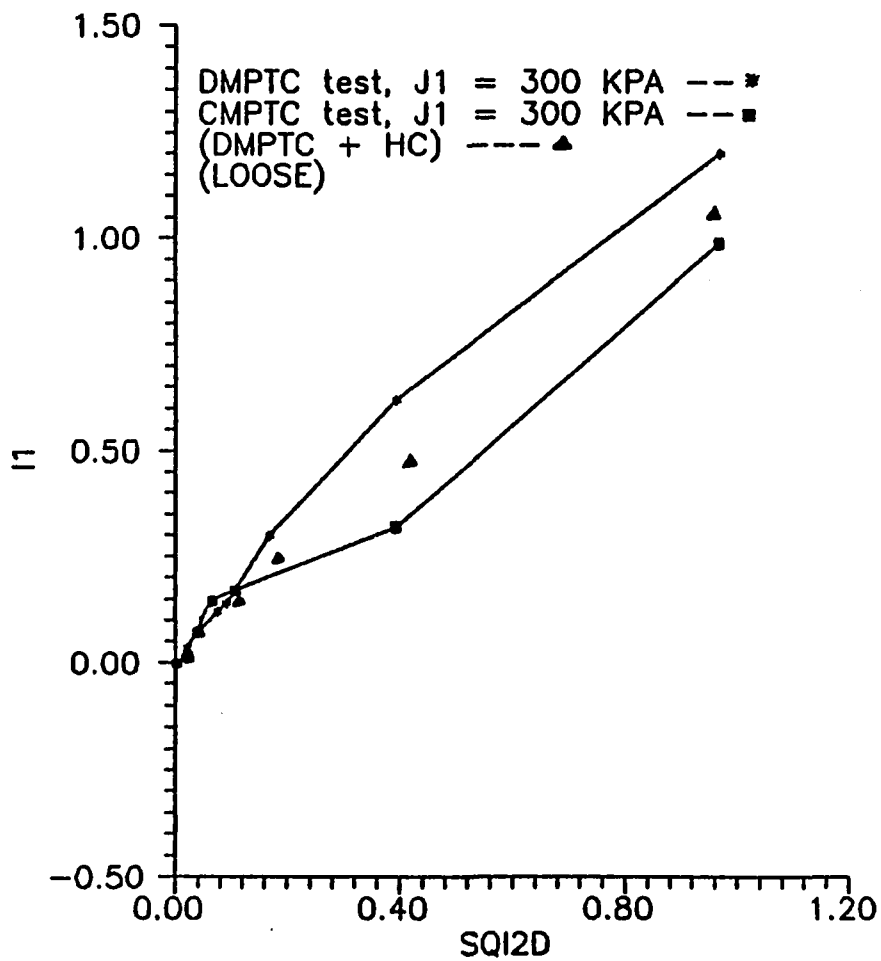


Figure 4.20. Comparison of Volumetric response between CMPTC and DMPTC  
 Test on LB Sand,  $J_1 = 300$  KPa (Loose).

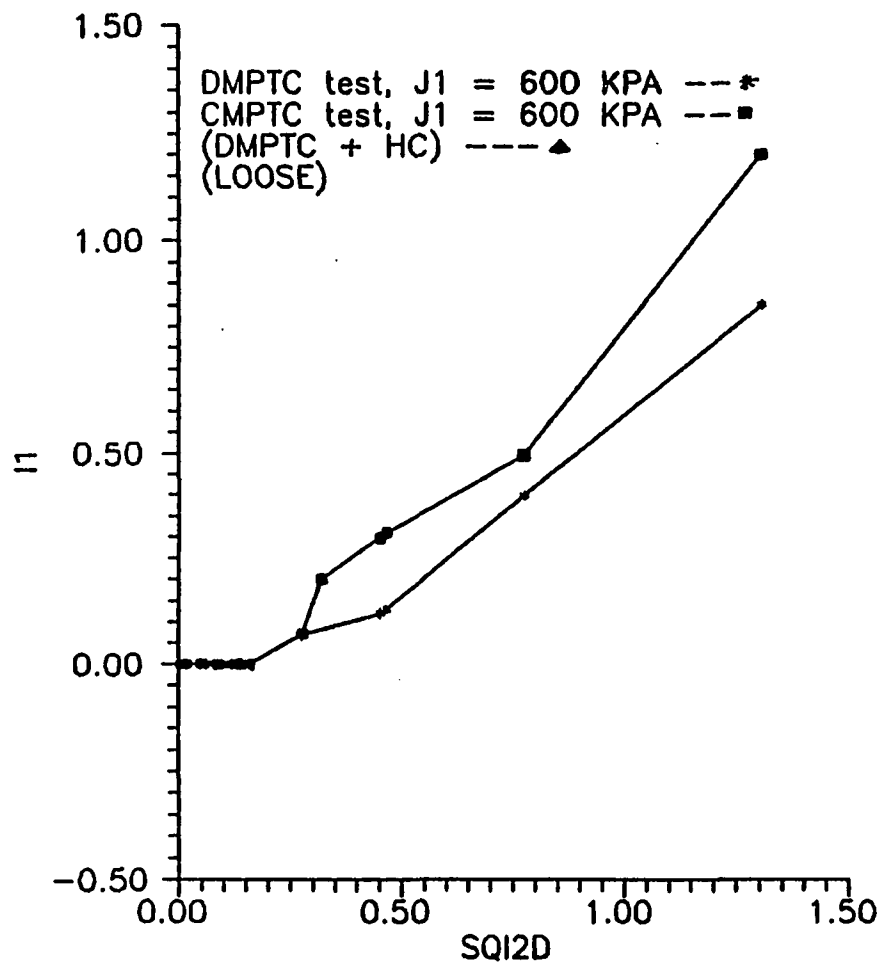


Figure 4.21. Comparison of Volumetric response between CMPTC and DMPTC Test on LB Sand,  $J_1 = 600$  KPa (Loose).

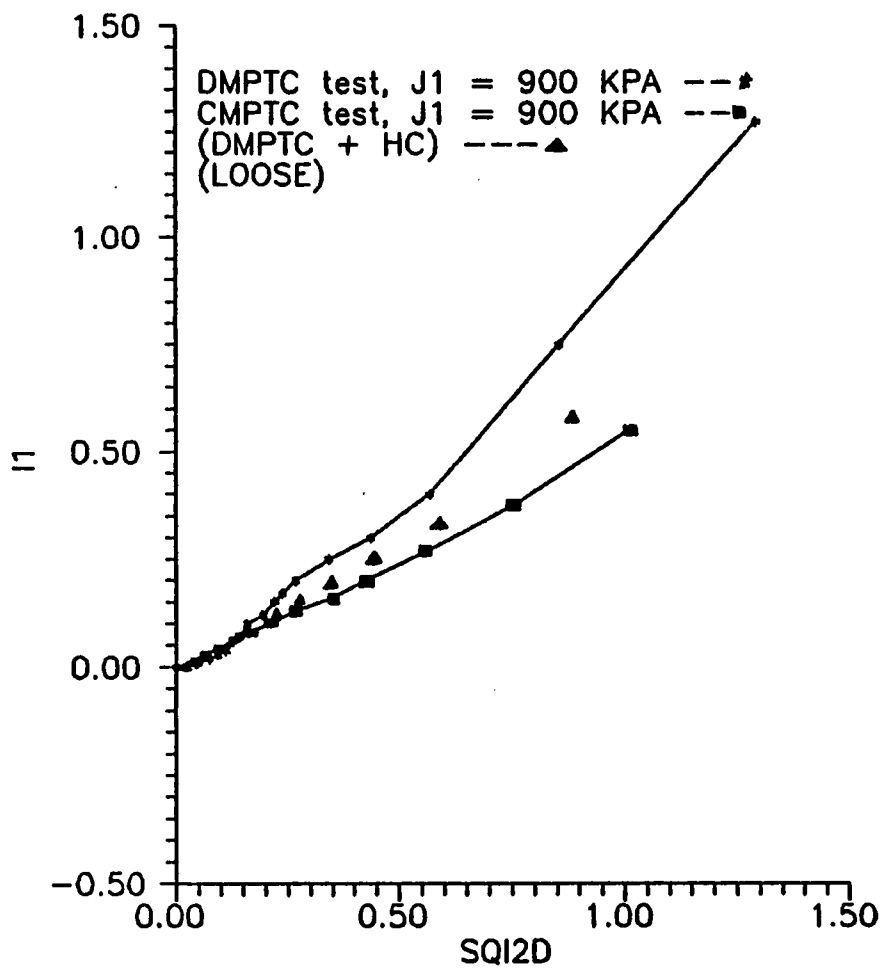


Figure 4.22. Comparison of Volumetric response between CMPTC and DMPTC  
 Test on LB Sand,  $J_1 = 900$  KPa (Loose).

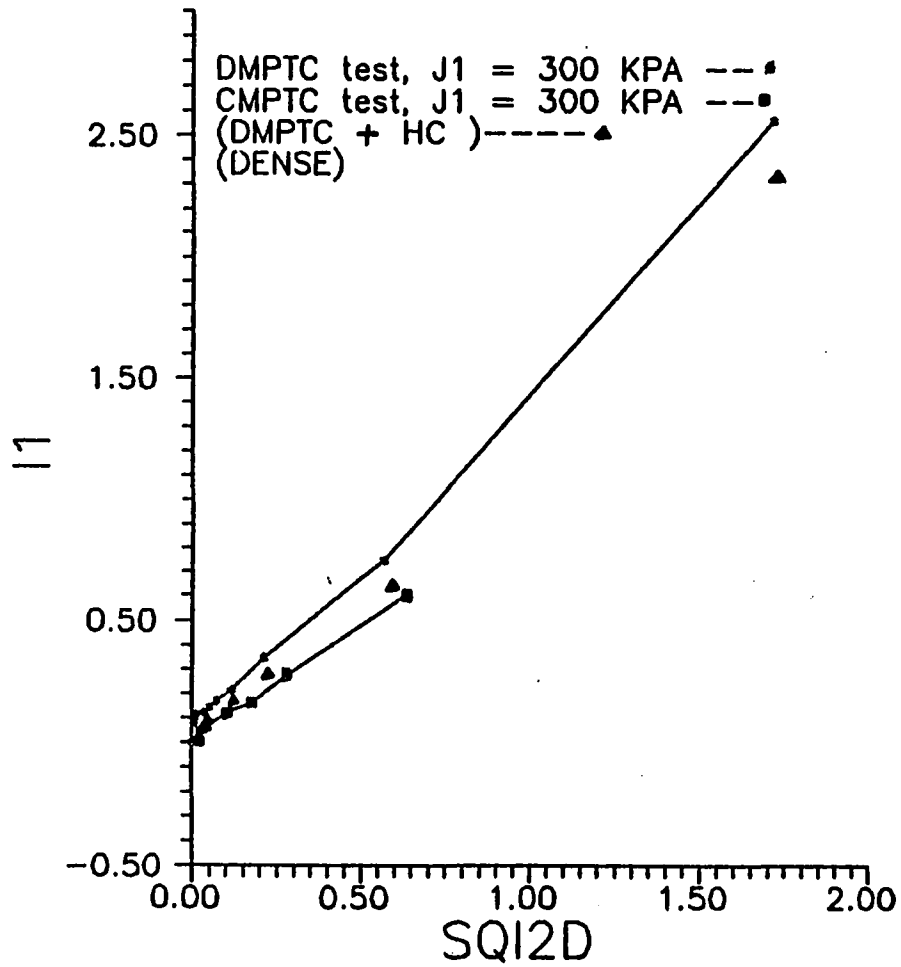


Figure 4.23. Comparison of Volumetric response between CMPTC and DMPTC  
 Test on LB Sand,  $J_1 = 300$  KPa (Dense).

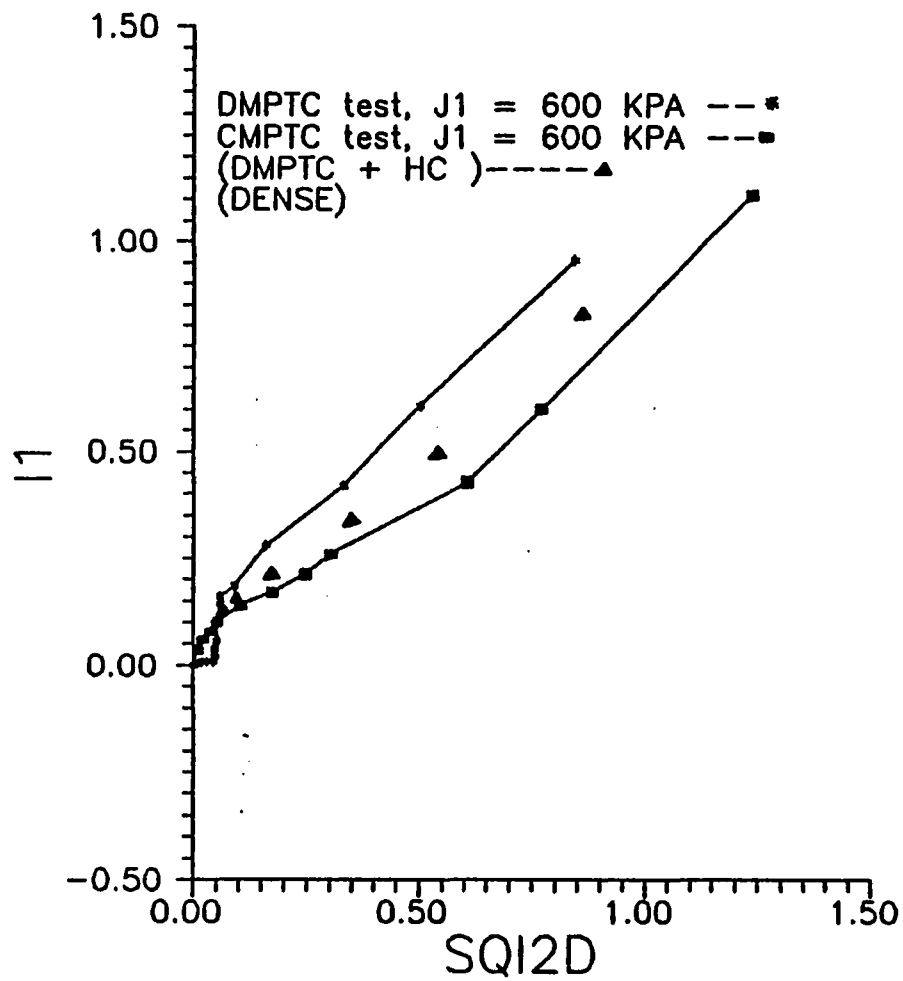


Figure 4.24. Comparison of Volumetric response between CMPTC and DMPTC  
 Test on LB Sand,  $J_1 = 600$  KPa (Dense).

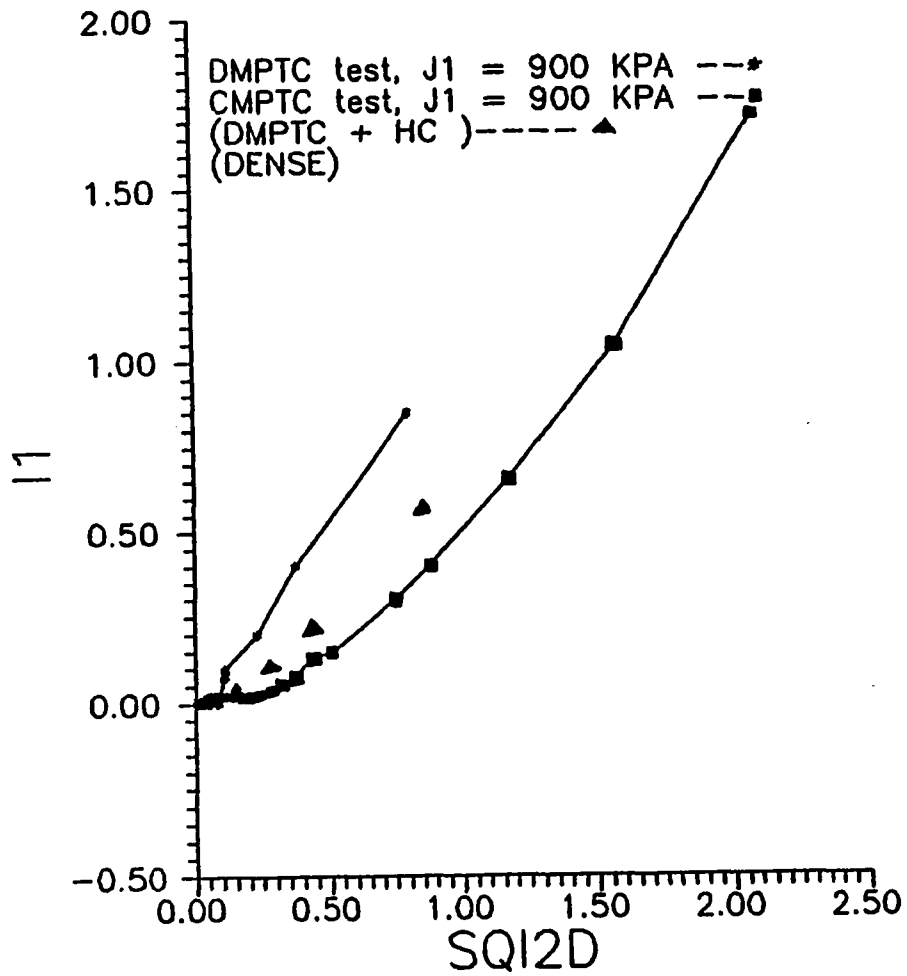


Figure 4.25. Comparison of Volumetric response between CMPTC and DMPTC Test on LB Sand,  $J_1 = 900$  KPa (Dense).

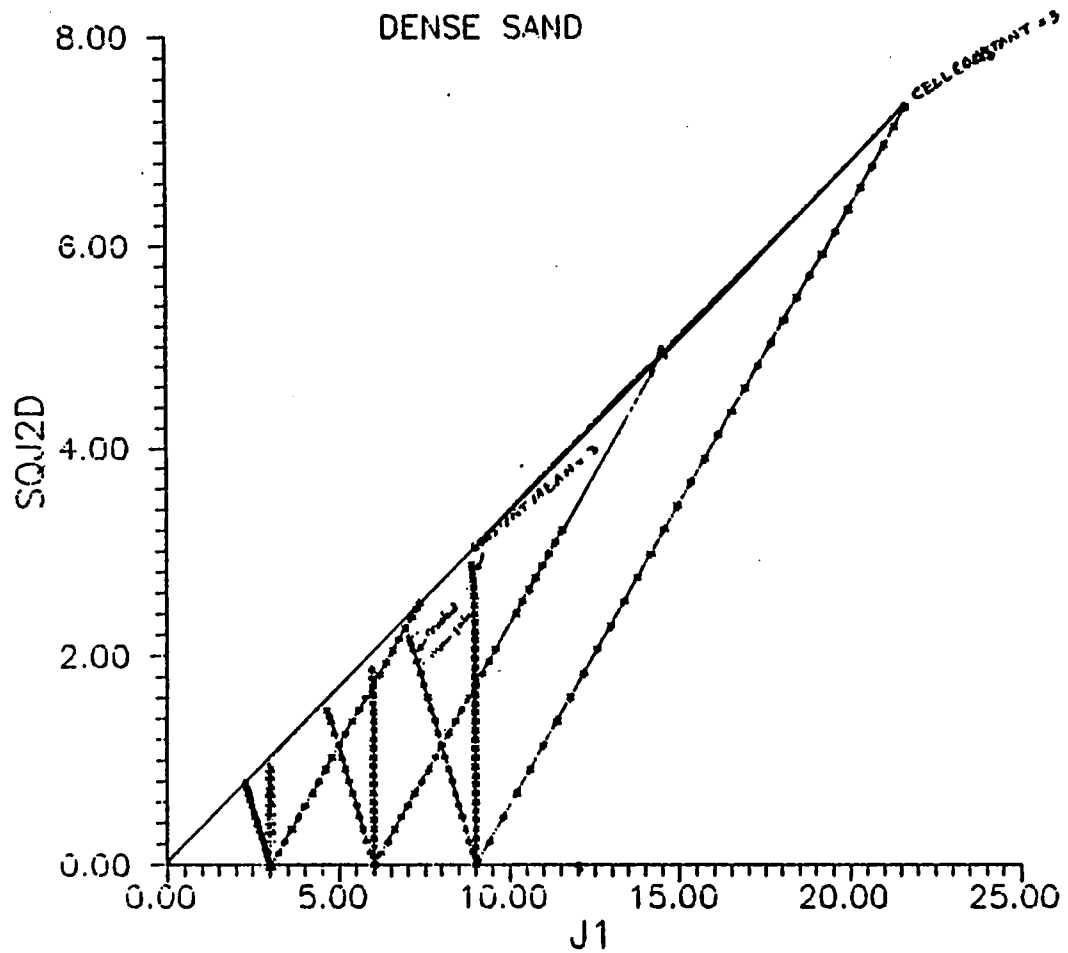


Figure 4.26. Plot of SQJ2D vs.  $J_1$  for CTC, CMPTC, and DMPTC Test on LB Sand.

$\sqrt{J_{2D}}$  and  $J_1$  from three types of tests are plotted on fig.4.26. From this figure it is observed that failure points for all type of tests under different confining pressures pass through one single straight line.

The three types of tests examined here have different stress paths on the  $J_1 - \sqrt{J_{2D}}$  plane. However, they have identical paths on the octahedral plane, ie.

they have the same Lode's angle. It is well known (Lade, 1987) that ultimate soil strength is path dependent. It is concluded here that the path dependency is restricted only on Lode's angle, while examining different paths on  $J_1 - \sqrt{J_{2D}}$  plane may be inconclusive.

#### 4.5 Summary of test results:

Effects of different parameters on shear and volumetric behavior of granular soils are investigated.

- 1) For CTC tests sand compresses at small strain and then dilates with the increase in shear strains. This dilation angle decreases as confining pressure increases.
- 2) For CMPTC and DMPTC tests dilation is observed from the beginning of shearing. Further observation lead us to believe that the compression observed in CTC tests is not due to shearing but due to increase in mean pressure.
- 3) Dilation angle also decreases with the initial confining pressure. Dilation after peak increases with a constant angle and it decreases as  $J_1$  increases.
- 4)  $\sqrt{J_{2D}}$  and  $J_1$  of three types of tests indicate that failure points for all

types of tests under different confining pressure pass through one single failure line. It is interesting to note that the experiments performed here had different paths on the  $\sqrt{J_{2D}} - J_1$  plane. However, they all had identical paths on the octahedrel plane ( e.g. Lode's angle was always the same). It has been demonstrated in previous investigations ( e.g. Hashmi, 1986, Lade and Duncan 1976) that tests performed using different stress path in the octahedrel plane resulted to different failure envelopes. Thus we conclude that Lode's angle is the only important feature of path dependency.

## 5. COMPARISON WITH PUBLISHED LITERATURE:

### 5.1 General

A number of investigators have performed series of experiments to examine soil behavior and used them to develop constitutive equations. Their data constitute a valuable source for further analysis under the scope of the present study. Some of these very important works are reviewed here.

Hashmi (1986) performed tests on LB sand using a true triaxial machine. Fig. 5.1 through 5.4 show stress-strain and volumetric response of two conventional triaxial compression (CTC) tests performed at 5.0 psi (34.45 KPa) and 13.0 psi (89.57 KPa), respectively. For both cases, relative density is 95% . It is observed that sand compresses initially, then dilates. Dilation is less for higher confining pressure. It is also shown clearly that dilation continues at a constant rate after the peak strength is achieved.

Fig 5.5 through 5.8 shows stress-strain and volumetric response of CMPTC test performed at initial confining pressures of 13.0 psi and 20.0 psi (137.8 KPa), respectively. For these tests, dilation starts from the beginning of application of deviatoric stress confirming the finding of the experimental program of the present study. Dilation for both CTC and CMPTC tests decreases for higher confining pressure.

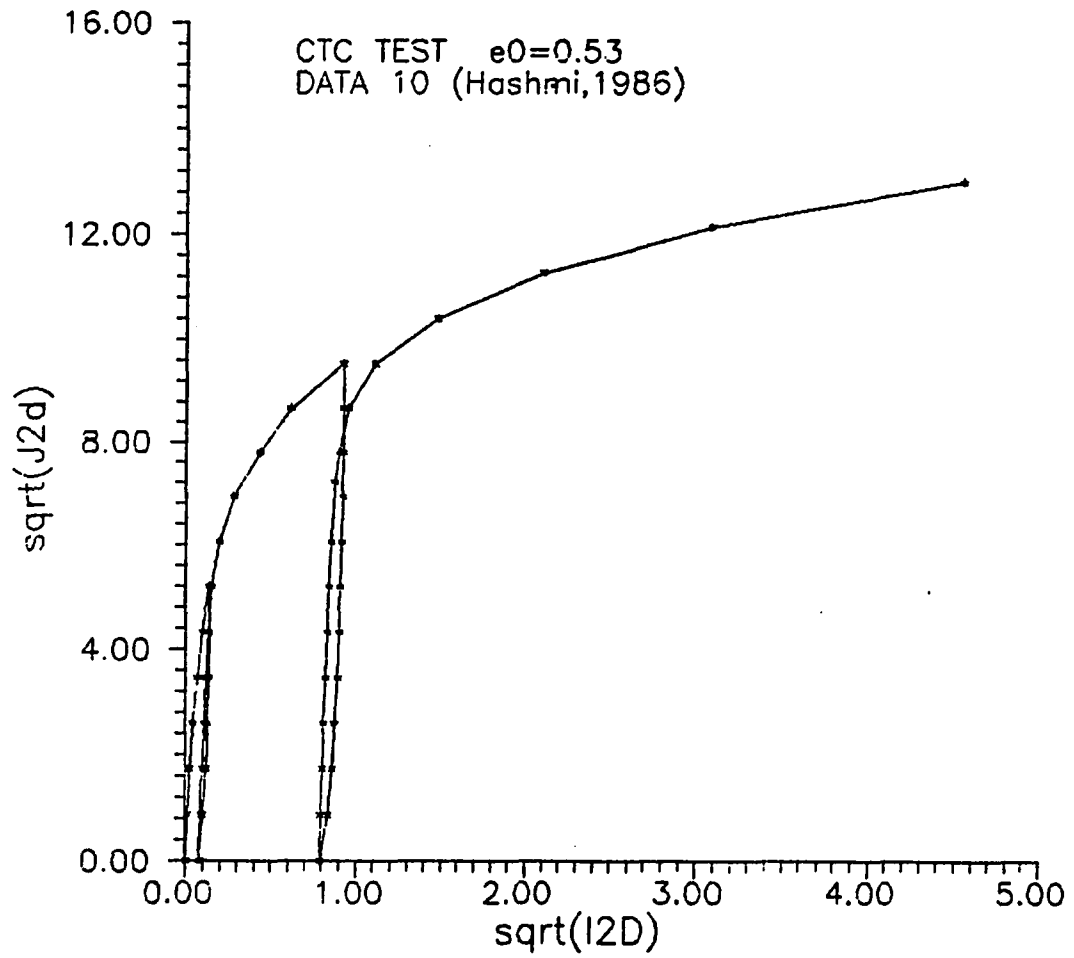


Figure 5.1. Stress-strain Response of CTC Test on LB Sand,  $\sigma_0 = 5$  psi (13.78 KPa), after Hashmi (1986).

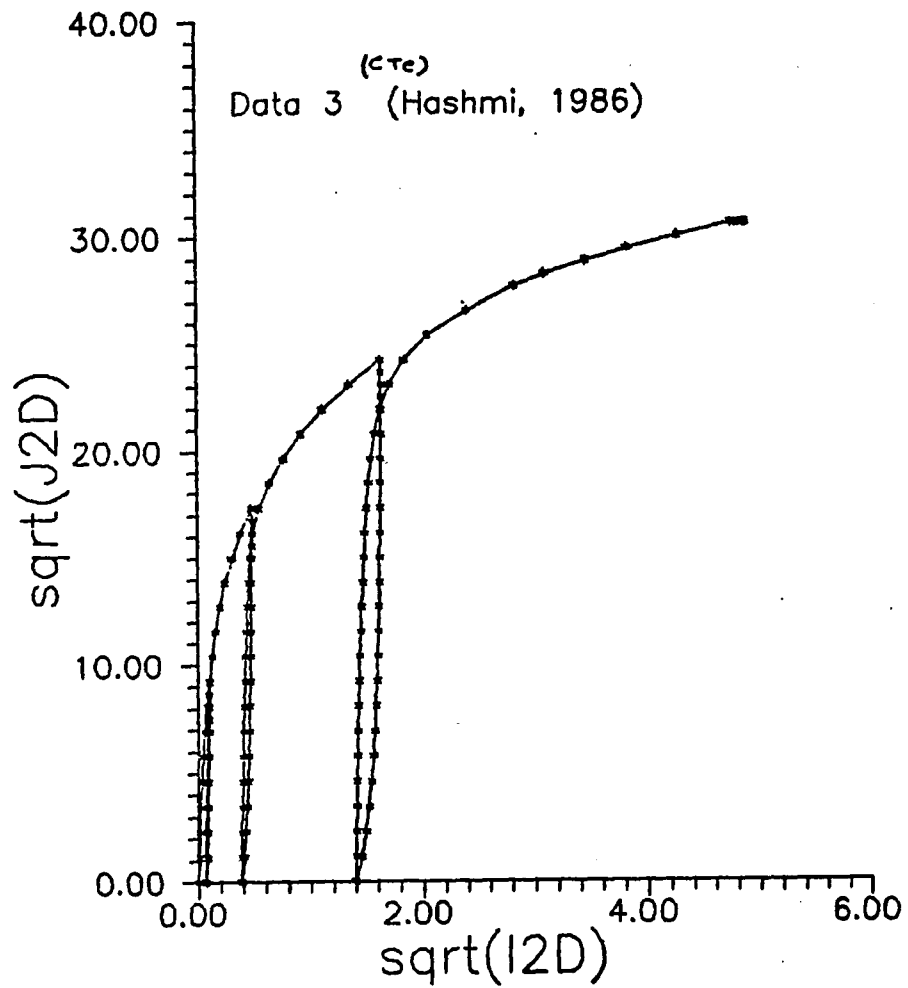


Figure 5.2. Stress-strain Response of CTC Test on LB Sand,  $\sigma_0 = 13$  psi (89.57 KPa), after Hashmi (1986).

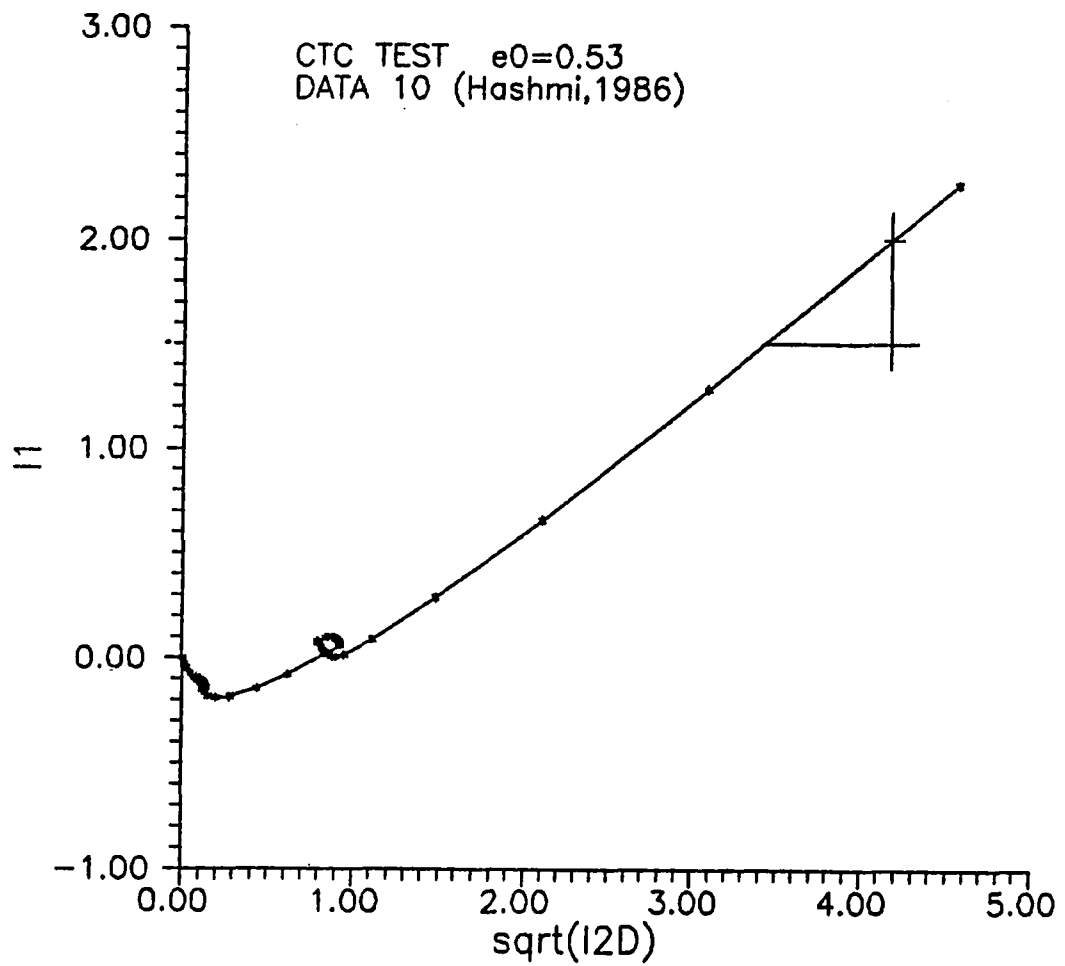


Figure 5.3. Volumetric Response of CTC Test on LB Sand,  $\sigma_0 = 5$  psi (13.78 KPa), after Hashmi (1986).

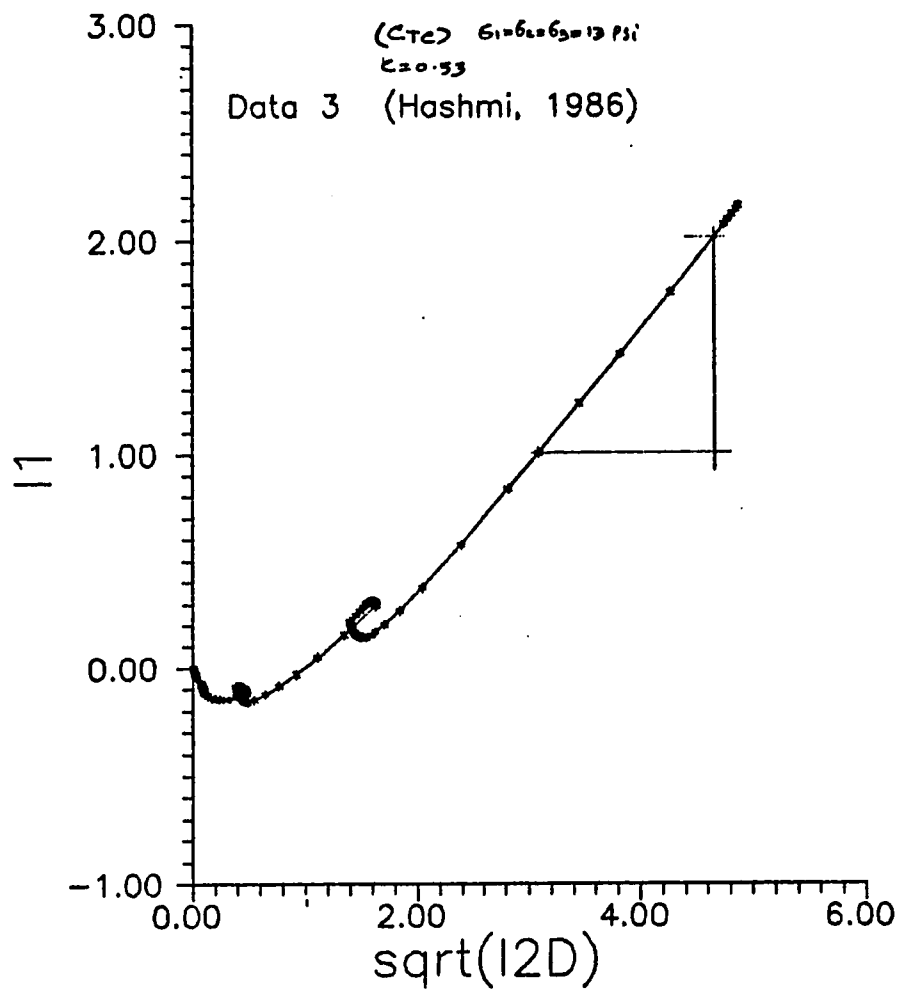


Figure 5.4. Volumetric Response of CTC Test on LB sand,  $\sigma_0 = 13 \text{ psi}$  (89.57 KPa), after Hashmi (1986).

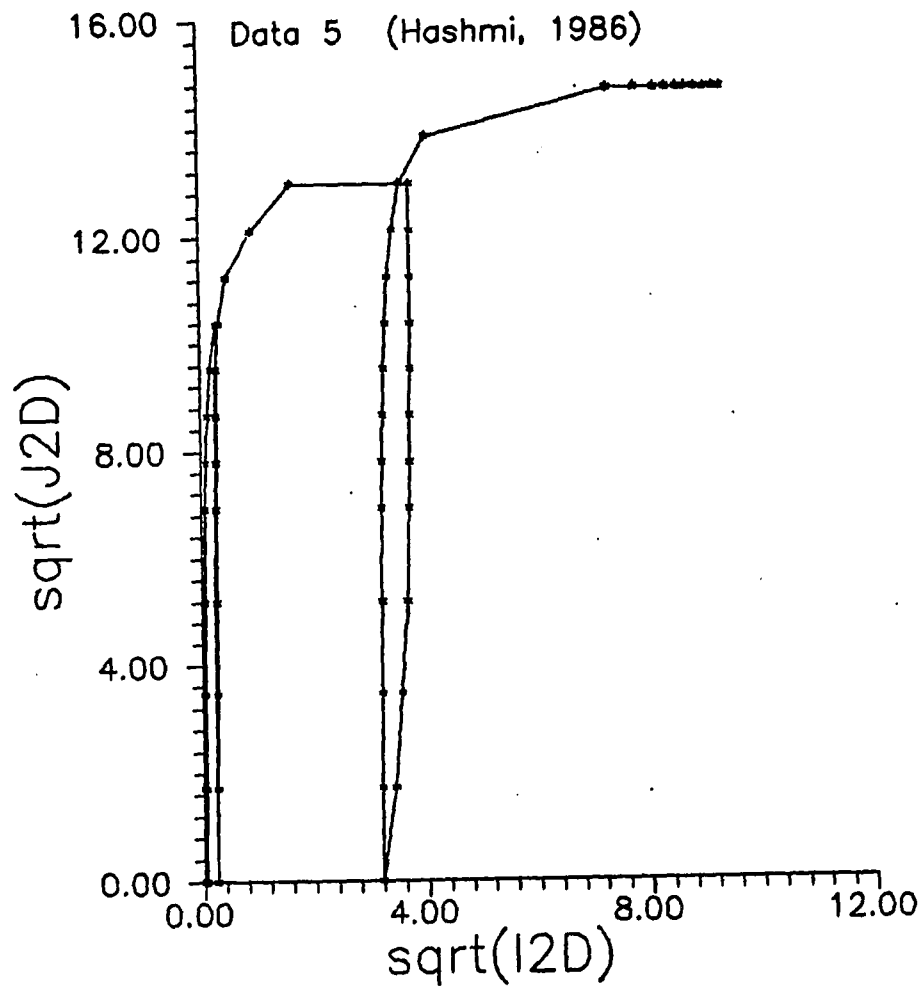


Figure 5.5. Stress-strain Response of CMPTC Test on LB Sand,  $\sigma_3 = 13$  psi (89.45 KPa), after Hashmi (1986).

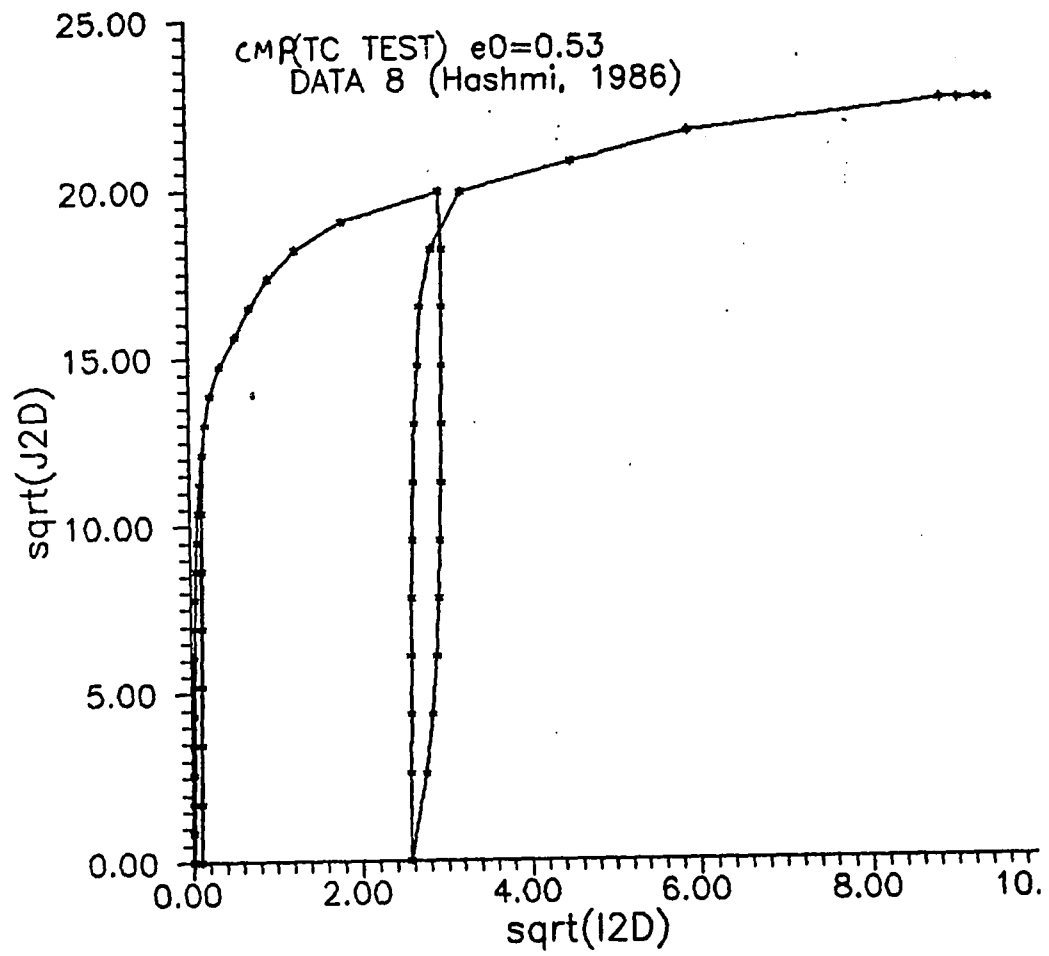


Figure 5.6. Stress-strain response of CMPTC Test on LB Sand,  $\sigma_3 = 20$  psi (137.8 KPa), after Hashmi (1986).

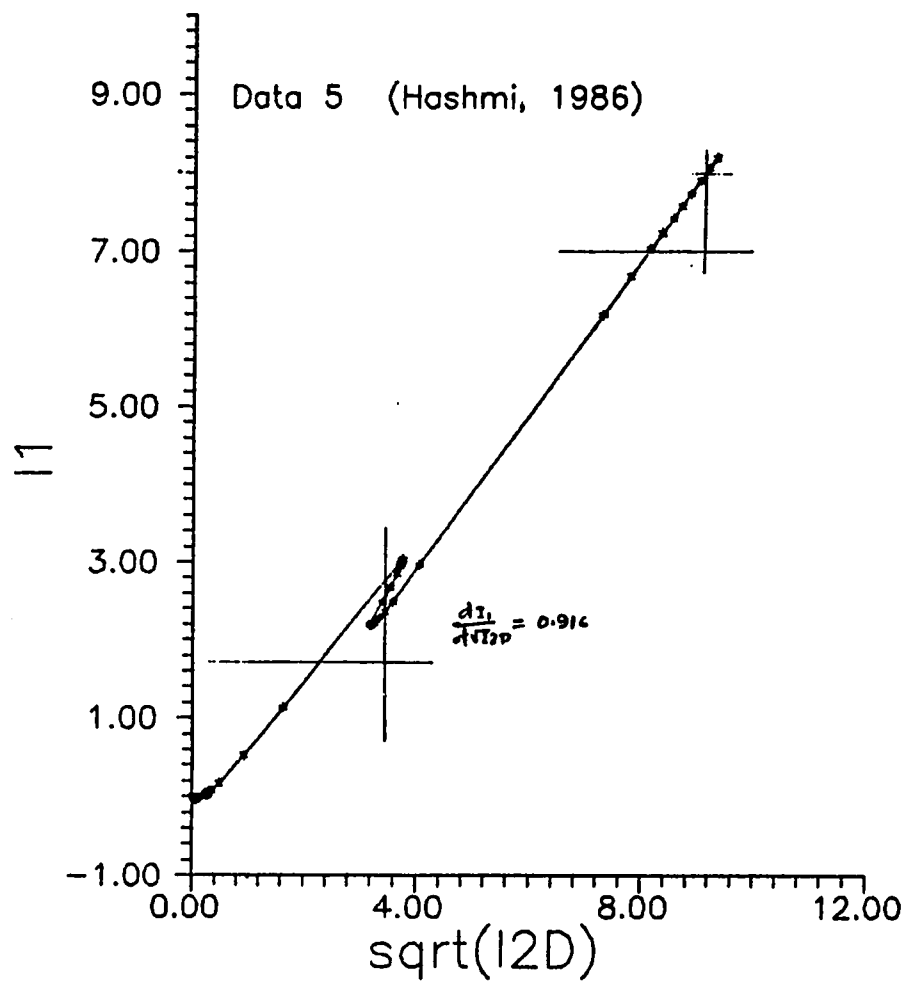


Figure 5.7. Volumetric Response of CMPTC Test on LB Sand,  $\sigma_3 = 13$  psi (89.45 KPa), after Hashmi (1986).

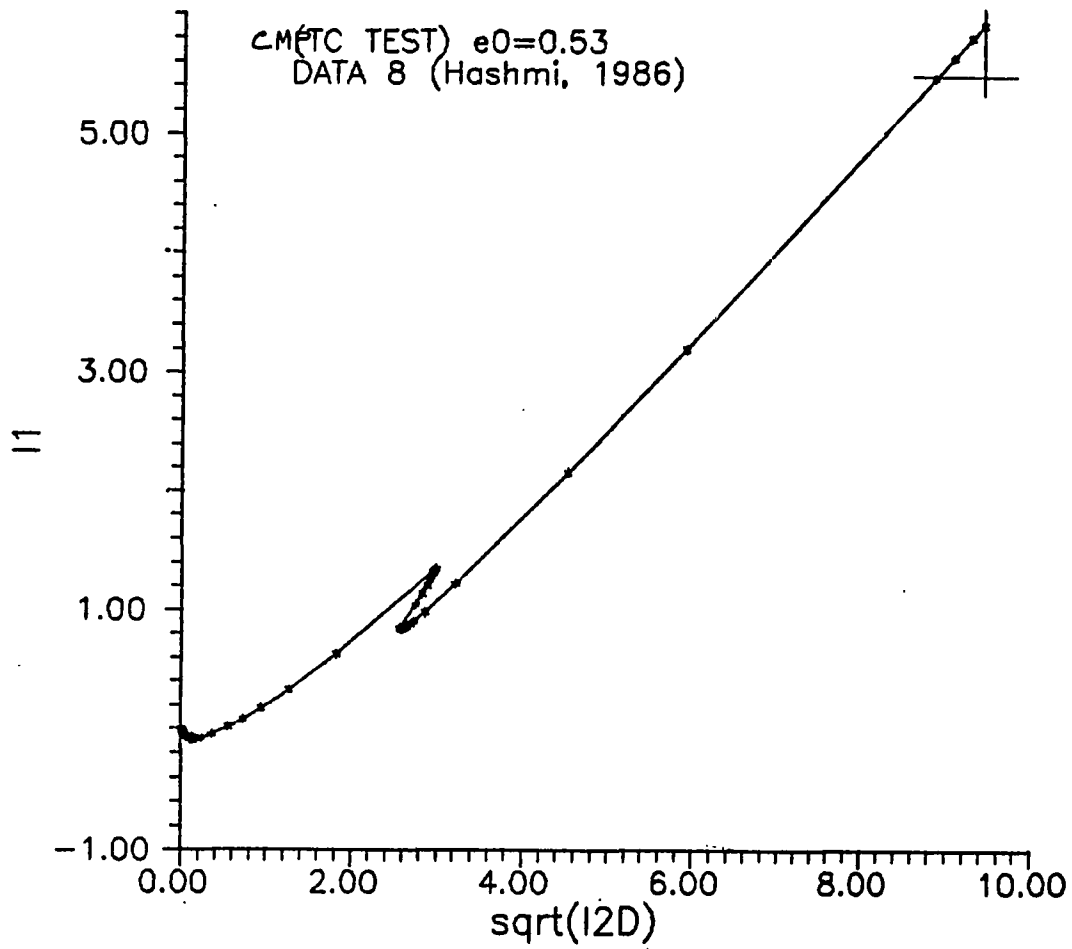


Figure 5.8. Volumetric Response of CMPTC Test on LB Sand,  $\sigma_3 = 20$  psi (137.8 KPa), after Hashmi (1986).

HASHMI-(1986), DR=25,35,45 & 65  
 CTC Test,  $\sigma_0 = 5 \text{ psi} (34.45 \text{ KPa})$

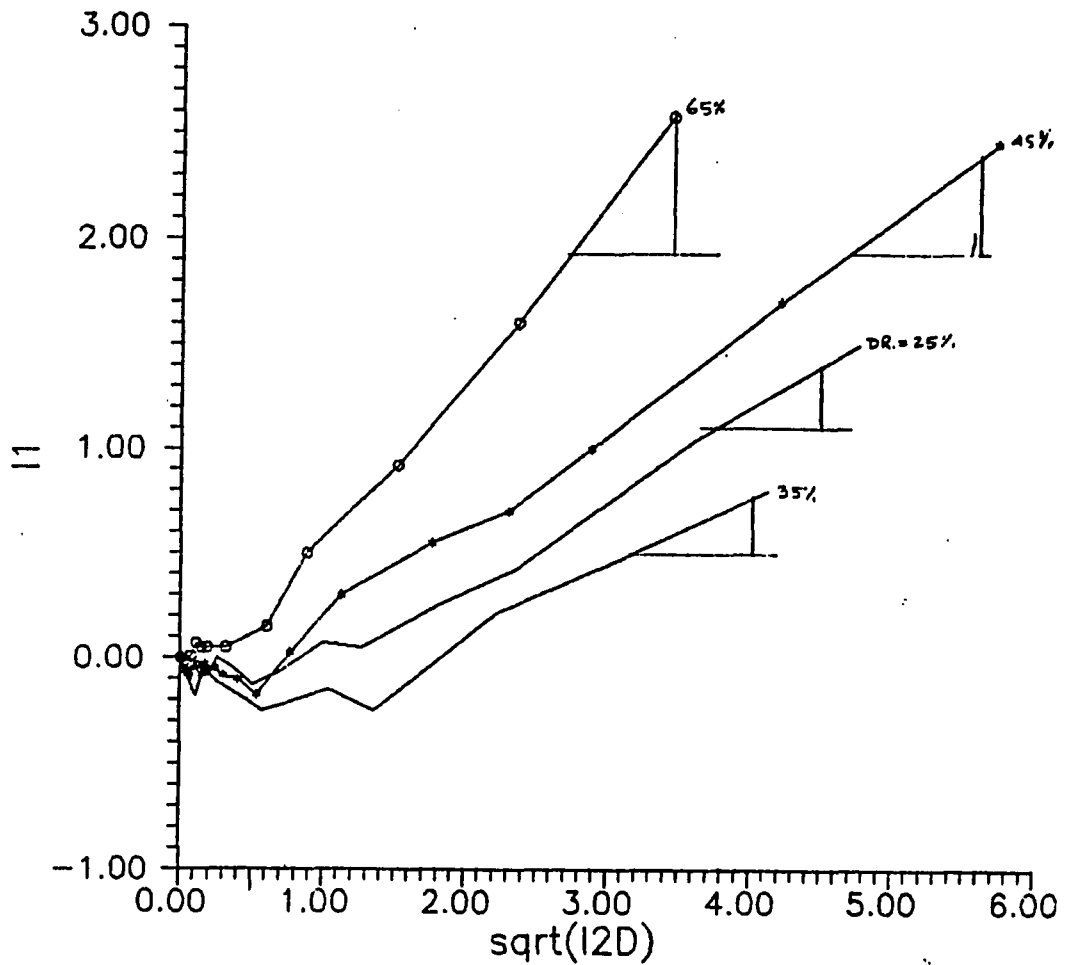


Figure 5.9. Volumetric response of CTC Test on LB Sand with Relative density  $D_r = 25\%$ ,  $35\%$ ,  $45\%$  and  $65\%$ , after Hashmi (1986).

Hashmi (1986) also performed CTC tests using different initial densities. It is found that as relative density increases dilation angle also increases ( fig.5.9).

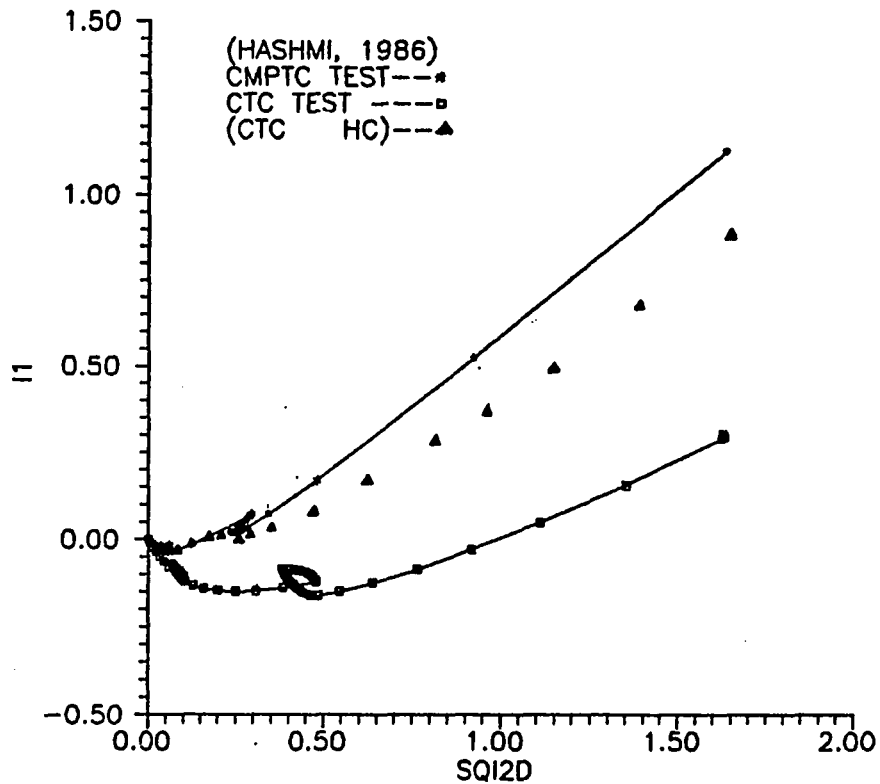


Figure 5.10. Comparison of volumetric Response of CTC and CMPTC tests on LB Sand,  $\sigma_0 = 13$  psi after Hashmi (1986).

Following the procedure used in the analysis of the experimental program of this study, CTC and HC results are combined to create the same stress path as the CMPTC test (figure 5.10). It becomes clear, that in the "elastic" region

$\left[ \sqrt{I_{2D}} < 0.5\% \right]$ , the results are identical, this suggesting that negative dilation is only due to increase of mean pressure. The same of course, was found from the analysis of our own experimental results, as is described in section 4.4.

Lee and Seed (1967) examined drained strength characteristics of sands. They observed that increase of confining pressure, reduces the brittle characteristics of the stress-strain curve, increases the failure strain, and decreases the tendency to dilate (fig. 5.11 ). The stress-strain volume change characteristics of dense sand at high confining pressures are like those of loose sand at low pressures. They also observed softening of soil and critical state behavior. After softening, steady state condition is observed. However, these results have led in the past to a different contradicting interpretations. A number of investigators used these results as evidence that soils exhibit softening and steady state flow. Reevaluation of such tests however, reveals that softening follows loss of uniformity of the sample deformations and initiations of shear band (a well defined thin zone of failure inclined approximately at  $45 + \phi/2$  degrees). When this occurs, the masses of the soil sample on both sides of the shear band slide with respect to each other as solid blocks while all the deformation occurs in the thin failure layer. What is observed then, is the failure of a structure rather than a uniformly loaded element. The load is thus distributed in a much smaller zone and the stress-strain recordings are no more representative of the material behavior. Similarly, while dilation occurs only in the shear band, the volumetric strain is calculated by dividing this volume change by the total volume of the sample. The result thus grossly underestimates the actual volumetric strain and the sample appears to flow under steady state.

The results of the present study, as well as the ones reported by Hashmi (1986), and as will be discussed later, by Lade (1973) and Vardoulakis (1984) indicate that for the entire range of reliable measurements, soils dilate constantly (steady state is not reached).

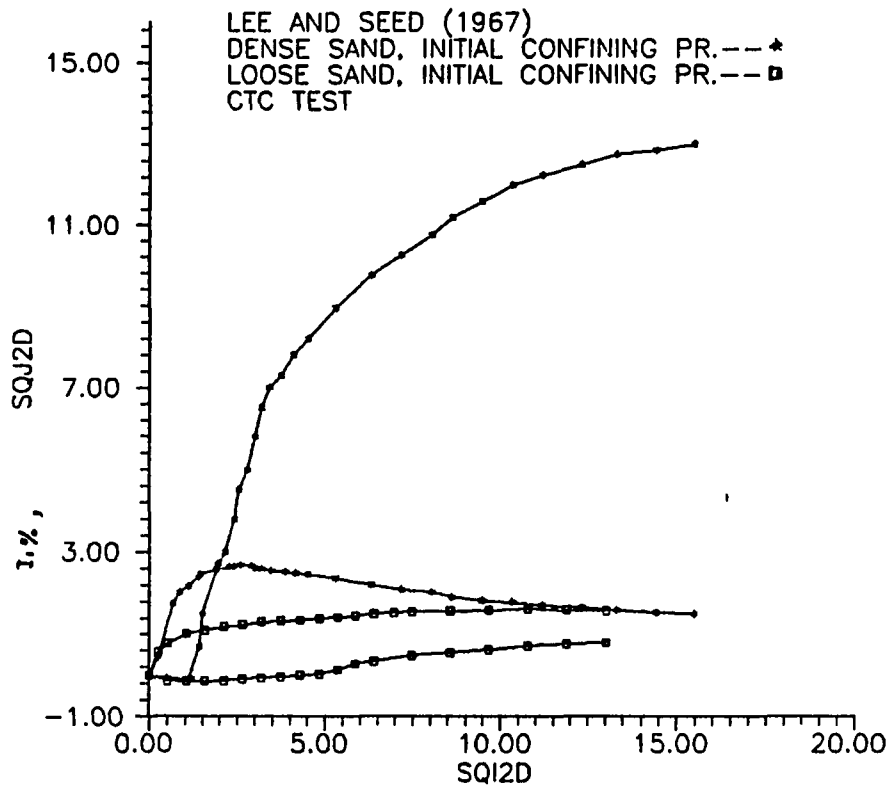


Figure 5.11. Stress-strain-volume change data of CTC Test on dense and loose sand, after Lee and Seed (1967).

Poul V. Lade (1973) also examined the effects of voids and volume changes on the behavior of frictional materials. Fig. 5.12 shows the results of a typical

drained triaxial compression test performed with constant confining pressure of 2 Kg/cm<sup>2</sup> on sand. The stress-strain relationship is non linear, and a small decrease in strength follows peak failure. This shows slight softening at large strain. However, the origin of softening here is different from the one observed in the results of Lee (1967). As will be discussed later, this is not due to structural failure of the sample, and should be incorporated in the constitutive model. The volumetric strain is initially compressive, but eventually the material dilates. Unfortunately, the results presented by Lade (1973) did not include other stress paths similar to the ones conducted in this study. As a result further comparisons are not possible.

Varadarajan et al.(1987) investigated the effects of stress-path on the stress-strain-volume change relationships of a river sand. They conducted a series of tests where the mean pressure was kept constant for half the test, and was subsequently reduced (figure 5.13). It is observed that dilation occurred from the very beginning of shearing, verifying once more that negative dilation observed in the CTC tests is due to the increased mean pressure.

Vardoulakis et al. (1984) examined the behavior of dry sand in a large triaxial apparatus. From fig.5.14 it is observed that dilation occurs at constant rate and that the slope of dilation decreases with confining pressure. This behavior is similar to the one observed in the current investigation.

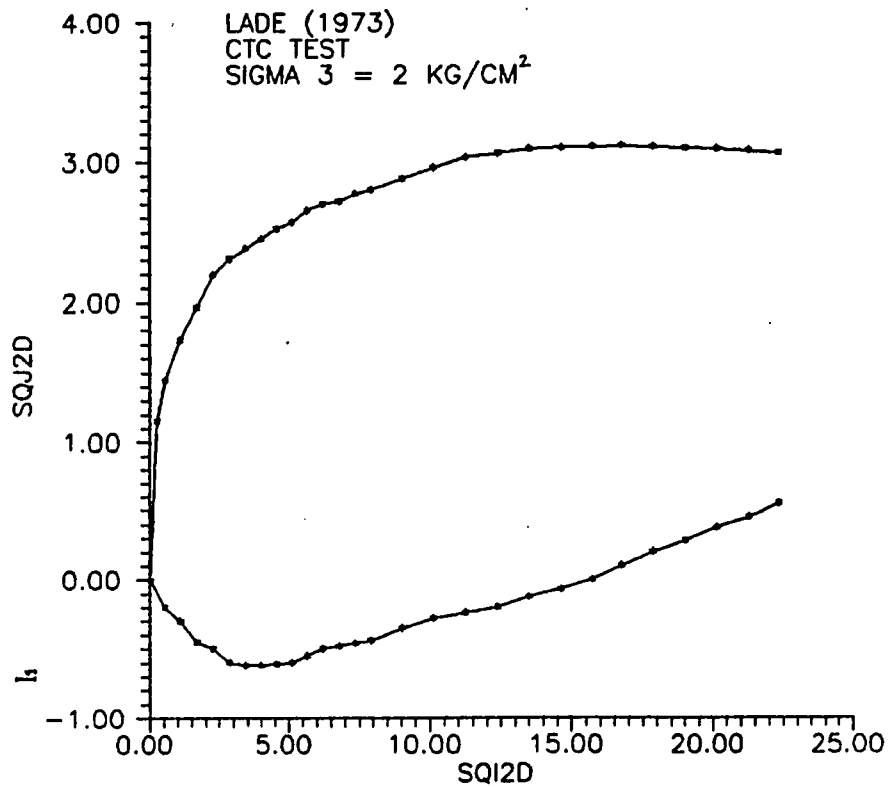


Figure 5.12. Stress-strain and volume change relations for drained triaxial compression test, after Lade, (1973).

### 5.2 Comparison and Conclusions:

Useful conclusions can be drawn from the results presented in the present study and the studies reviewed here. Some of the observations are well known but are repeated here for completeness.

All tests examined here show dilation increase with mean pressure decrease and density increase. A more interesting conclusion and probably one to be debated by other researchers, is that shearing under constant or decreasing mean pressure

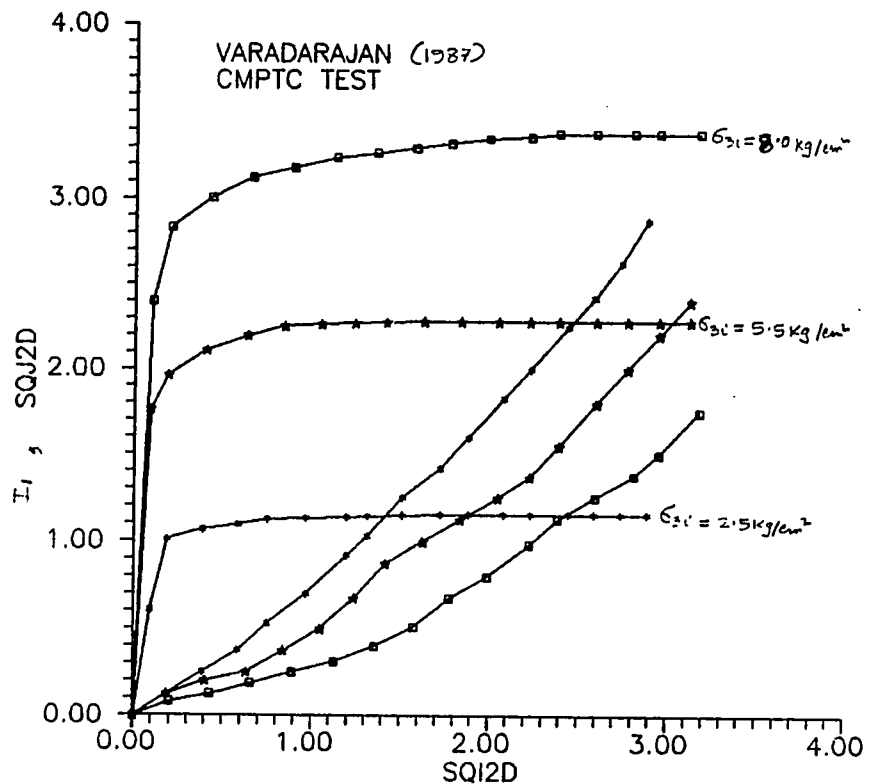
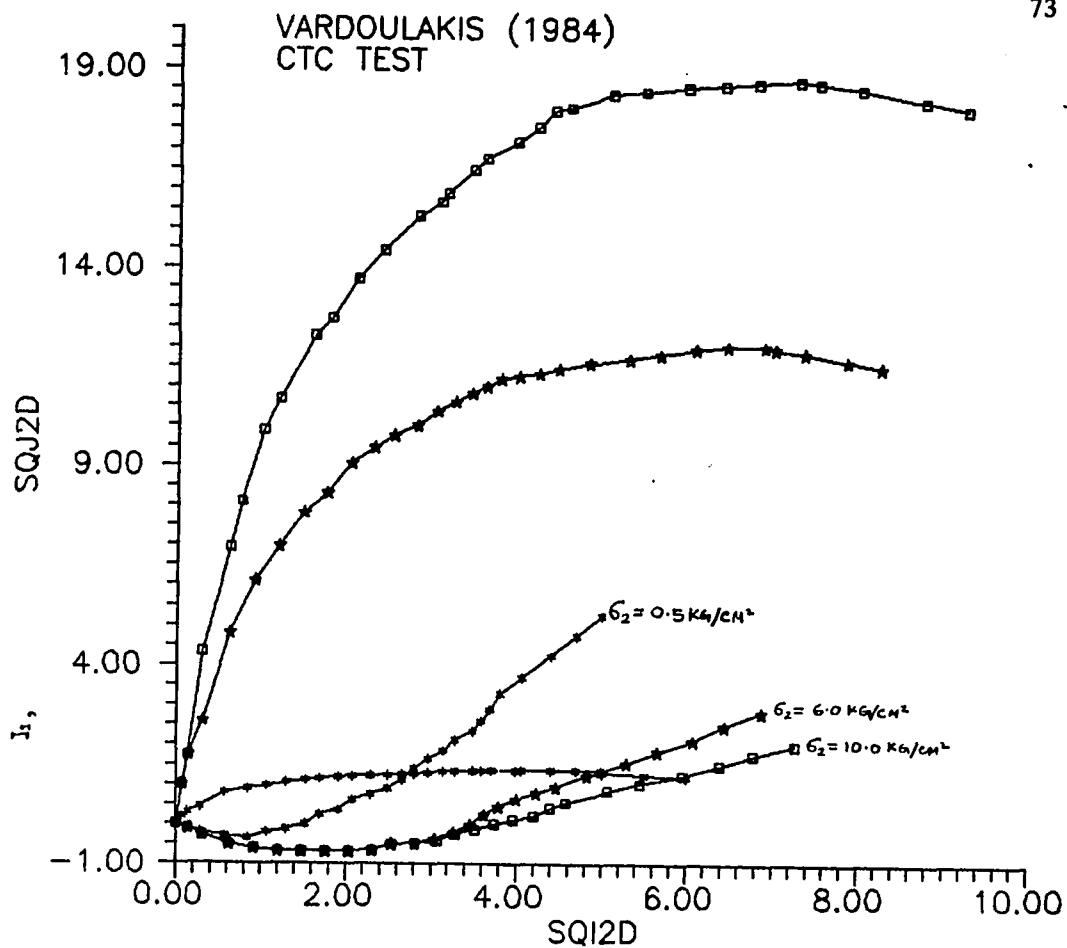


Figure 5.13. Stress-Strain-Volume change relationship, after Varadarajan et al.(1987).

is accompanied by strict dilation (no volumetric compression). This conclusion is affirmed by the observations of a number of researchers. It is also verified by indirect observations where it is proved that in the "elastic" range of soil deformations (small strains) the volumetric strains of shearing test differ from those of another test by the amount corresponding to their to their difference of mean pressure. As a result of this observation it is concluded that volumetric compression observed in the early stages of CTC tests is due to the increase of



mean pressure.

Another important conclusion of this study is that dilation is constant after shear failure and that steady state is not achieved for the entire range of useful strain measures.

Finally, an important observation that merits discussion here is the slight softening observed after the peak strength is achieved. It is well known that the ultimate strength of granular materials increases as density increases. The sample reaches failure no further stress increase is possible at a certain strain.

Further loading produces more dilation which decreases the density of the sample, thus "shrinking" the failure surface (i.e.  $\phi$  decreases). This results to the slight softening that is observed after failure.

As opposed to the softening observed in Lee's testing which is caused by structural failure of the specimen, this is material softening and should be incorporated to the constitutive modeling of the material.

Since different stress paths cause different dilation characteristics, the decrease of strength due to dilation may be partly responsible for small differences in friction angle for different stress paths.

## 6. SUMMARY AND CONCLUSIONS

The behavior of geologic materials is nonlinear, inelastic and affected by factors such as state of stress, density and stress path. The work carried out in this study and the conclusions drawn from it may be summarized as follows.

1. From HC tests it is observed that both loading and unloading curves are highly nonlinear.
2. The upward trend of the stress-strain curve with increase of confining pressure suggests that material stiffens under pure hydrostatic state of stress. This behavior is also observed by other researchers, Lee 1967, Hashmi 1986, Lade 1987 and Varadarajan 1987.
3. It is found that in CTC tests, during shearing, sand compress at small strain and subsequently dilates with the increase in shear strains. For dense sands, dilation initiates at smaller shear strains than for loose sands because there are less voids to compact. This dilation continues at a steady rate beyond peak failure, and dilation angle for CTC test decreases with confining pressure.
4. For CMPTC and DMPTC tests sand dilates from the beginning of shearing. Comparison of the two tests (CMPTC and DMPTC) suggests that the initial volume compression observed in CTC test is predominantly due to the increases of mean pressure. If  $\Delta J_1 \leq 0$  then no negative dilation occurs. This behavior is also observed by other researchers, (Hashmi 1986, and Varadarajan 1987).
5. The three type of tests examined in this study have different stress paths on the  $J_1 - \sqrt{J_2D}$  plane. However, they have identical paths on the octahedral plane ie. they have the same Lode's angle. It is concluded that stress path

dependence cannot be expressed on the  $J_1 - \sqrt{J_{2D}}$  plane.

6. Triaxial testing results to a slight softening due to the continued dilation of the sample after failure.

## LIST OF REFERENCES

- Baker, R. and Desai, C.S., "Consequences of Deviatoric Normality in Plasticity With Isotropic Strain Hardening," Int. J. Num. Analyt. Methods in Geomech., Vol. 6, No. 3, 1982, pp.383-390.
- Baltov, A. and Sawczuk, A., "A Rule for Anisotropic Hardening," Acta Mech., Vol. 1, N. 2, 1965, pp. 81-92.
- Baron, E. H., "A theory for the Mechanical Behavior of Sand," Proc., 11 th Int. Cong. Appl. Mech., 1964, pp. 163-191.
- Christian, J. T. and Desai, C. S., "Constitutive laws for Geological Media," Num. Methods in Geotech. Engg., McGraw-Hill Book CO., New York, 1977.
- Christian, J. T., Haggmann, A. J. and Marr, W. A., "Incremental Plasticity Analysis of Frictional Soils," Int. J. for Num. and Analyt. Meth. in Geomech., Vol. 1, 1977, pp. 343-375.
- Desai, C. S., "A General Basis for Yield, Failure and Potential Functions in Plasticity," Int. J. Num. analyt. Meth. in Geomech., Vol. 4, 1980, pp. 361-375.
- Desai, C. S. and Christian, J. T. (Eds.), Numerical Methods in Geotechnical Engineering, McGraw-Hill, New York, 1977.
- Drucker, D. C., Gibson, R. E. and Henkel, D. J., "Soil Mechanics and Work Hardening Theories of Plasticity." Trans., ASCE, Vol. 122, 1957, pp. 338-346.
- Hashmi, Q. S. E., "Non Associative Plasticity Model for Cohesionless materials and its Implementation in Soil-Structure Interaction," Ph.D. Dissertation, University of Arizona, Tucson, Arizona, 1983.
- Lade, P. V., "Elasto-Plastic Stress-Strain Theory for Cohesionless Soil with Curved Yield surfaces," Int. J. Solid Struct., Vol. 13, 1977, pp. 1019-1035.
- Lade, P. V. and Duncan, J. M., "Cubical Triaxial Tests on Cohesionless Soil," J. Soil Mech. Found. Div., ASCE, Vol. 99, SM 10, 13, pp. 793-812.

- Lade, P. V. and Duncan, J. M., "Stress Path Independent Behavior of Cohesionless Soil," J. Geotech. Engg. Div., ASCE, Vol. 102, GT 1, 1976, pp. 51-68.
- Lee, K. L., and Seed, B. H., "Drained Strength Characteristics of Sands," J. Soil Mech. Found. Div., ASCE, Vol. 93, No. SM6, 1967, pp. 117-141.
- Rad. N. S. and Tumay, M. T., "Factors Affecting sand specimen preparation by Raining," Geotechnical Testing Journal, GTJODJ, Vol. 10, No. 1, March 1987, pp. 31-37.
- Varadarajan, A. and S. S. Mishra, "Effect of Stress-Path on the Stress-Strain-Volume change Relationships of a River Sand," Third Australia-New Zealand Conference on Geomechanics, Vol.1-3, 1980.
- Vardoulakis, A. Hettler, "Behaviour of dry sand tested in a large triaxial apparatus," Geotechnique, Vol. 34, No. 3, 1984, pp.183-198.